Panoscopic Assembling of Ceramic Materials for Environmental Clean-up and Human Health

Tsugio Sato
Institute of Multidisciplinary Research for Advanced Materials,
Tohoku University,
Sendai 980-8577, Japan

TOHOKU UNIVERSITY

Symposium on Advanced Composite Materials
24 February, 2011
Sendai

MRAM TAGEN

CONTENTS

- Panoscopic Assembling of Ceramic Materials for High Performance Application
- Design and Development of Photocatalyst for Environmental Clean-up
- Design and Development of Ceria-based Inorganic UV-shielding Materials for Human Health
- Conclusion

- Panoscopic Assembling of Ceramic Materials for High Performance Application
- Design and Development of Photocatalyst for Environmental Clean-up
- Design and Development of Ceria-based Inorganic UV-shielding Materials for Human Health
- Conclusion

Panoscopic Assembling of Ceramics

Hierarchical morphology control of ceramics from nano

Nano Micro Bulk

Crystal growth

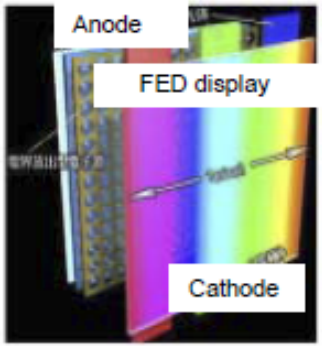

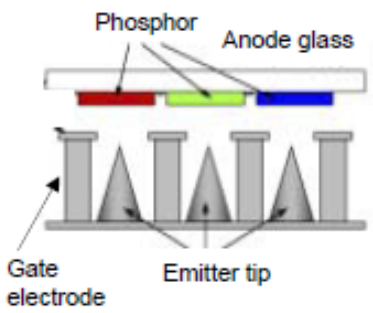

The constitution of the emission of light layer

FED display

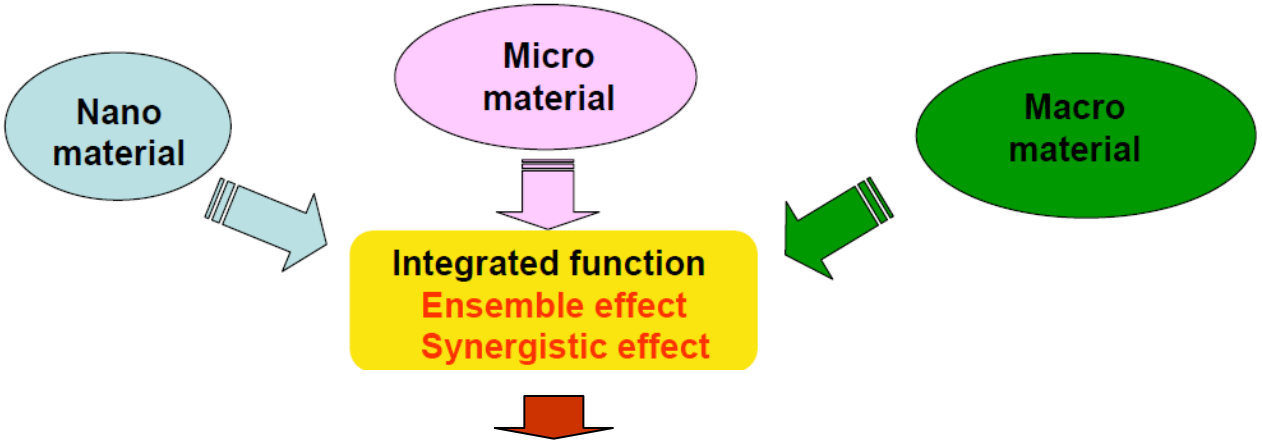

High Performance Photocatalyst for Environmental Clean-up
&
High Performance Inorganic UV-shielding Materials for Human Health

- Panoscopic Assembling of Ceramic Materials for High Performance Application
- Design and Development of Photocatalyst for Environmental Clean-up
- Design and Development of Ceria-based Inorganic UV-shielding Materials for Human Health
- Conclusion

Materials Chemistry to support Sustainable Development of Human Being Society

- Development of non-fossil energy using processes
- Efficient use of energies
- Effective production of the non-fossil energies

Global warming

Environmental pollutions

Drying up of resources

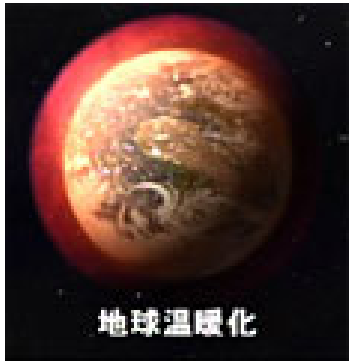

Photocatalytic reaction

Visible light
< 3 eV
(λ > 400 nm)

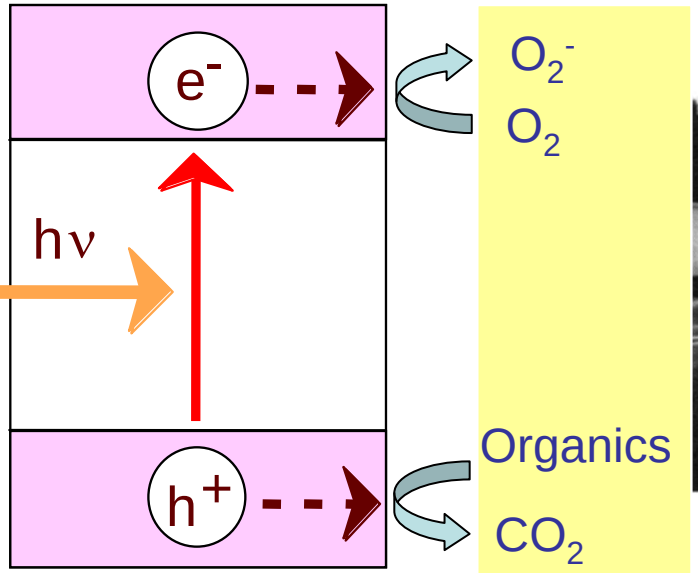

DeNO$_x$ catalyst
(Environmental clean-up)

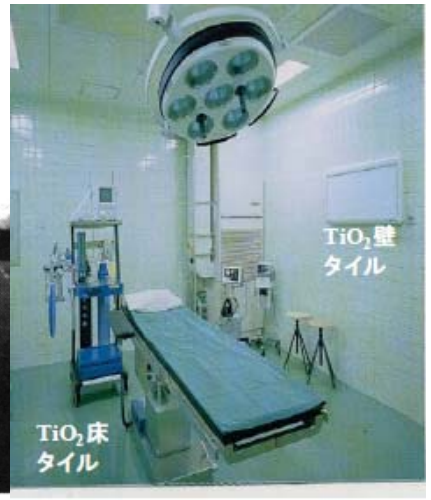

Antibacterial tile
(Toto Co.)

Anti-fogging

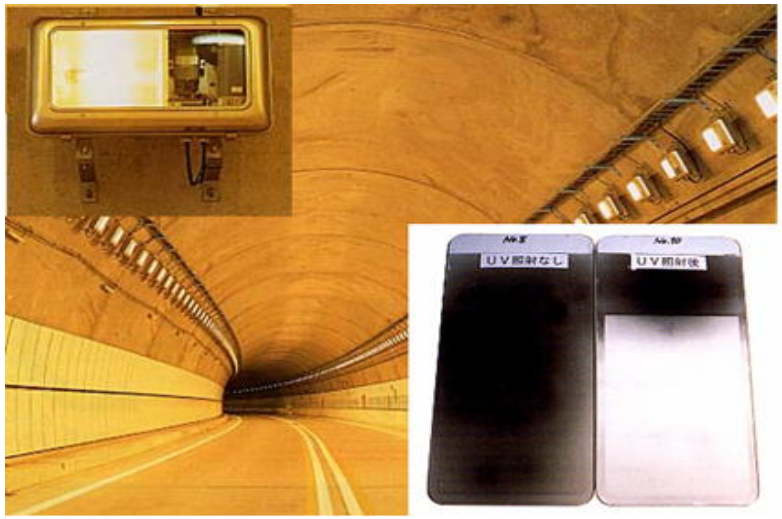

Self-cleaning of light cover glass in the tunnel of highway (Toshiba Lighting & Technology Co.)

Development of high performance visible light responsive photocatalyst which can use sunlight and/or indoor light

Design of high performance visible light responsive photocatalyt

Narrow band gap	⇒	Visible light use
High specific surface area	⇒	High contact efficiency
High crystallinity	⇒	Long life time of electron & hole
Composite formation	⇒	Long life time of electron & hole

High crystallinity fine particles of narrow bandgap semiconductors

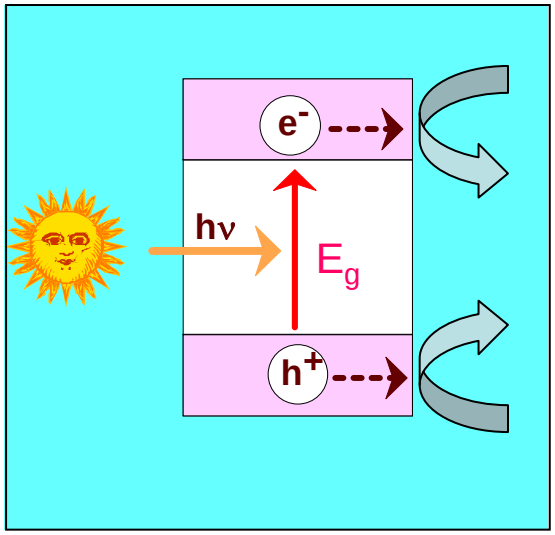

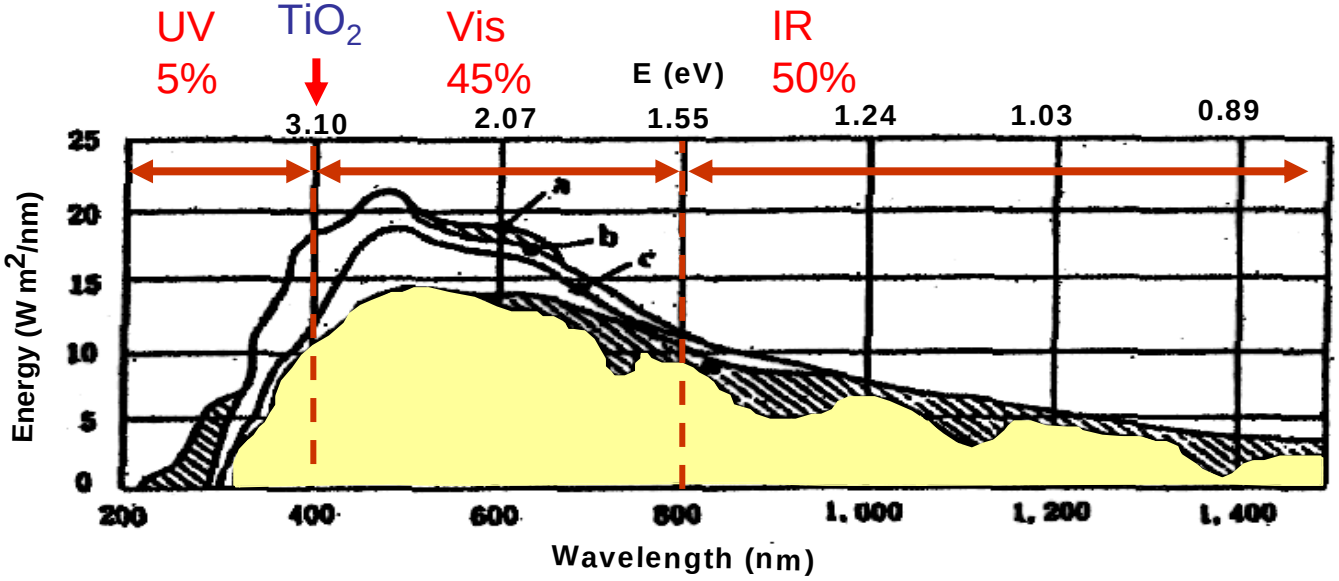

Spectra of sun light

Solvothermal reactions

Solvothermal

Solvent + Thermal

The First International Conference on Solvothermal Reactions
(1994, Takamatsu)

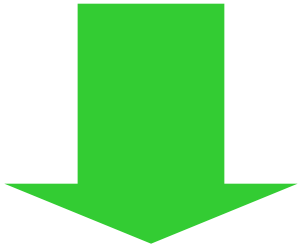

Reactions using high temperature and/or high pressure solvents

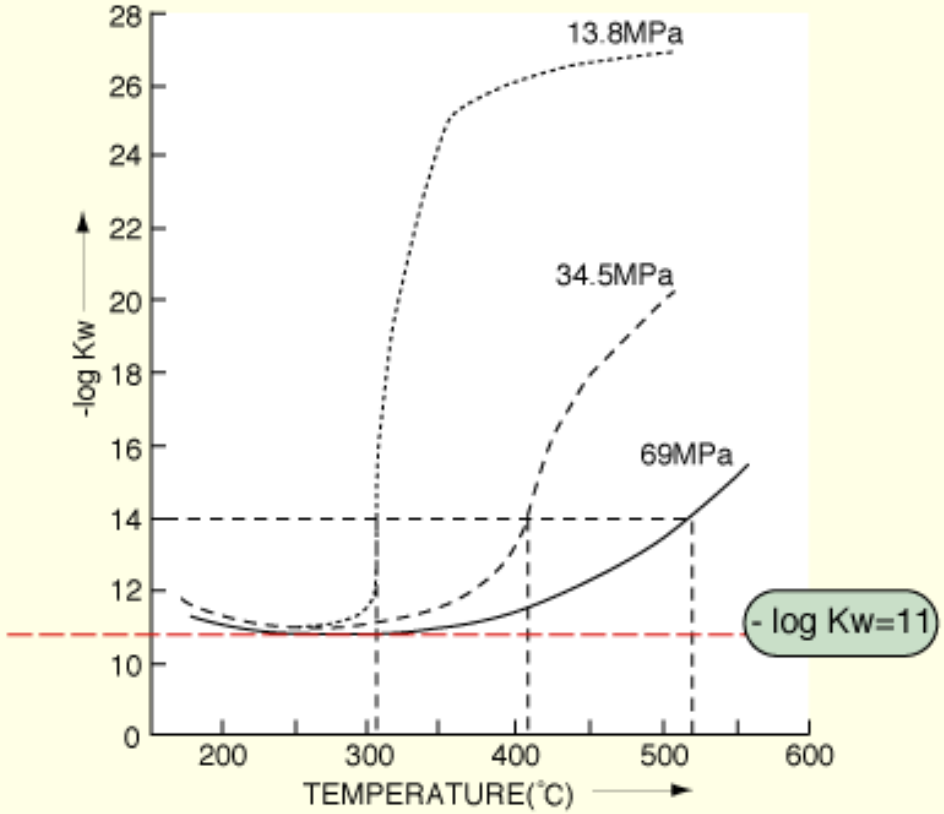

図１　水のイオン積

(1) 圧力/温度条件により
イオン積が大幅に変化

電解質溶媒としてイオン的反応場に
好都合な反応場を提供

解離が進み水自体が酸やアルカリの機能を示し、
加水分解作用が大きくなる

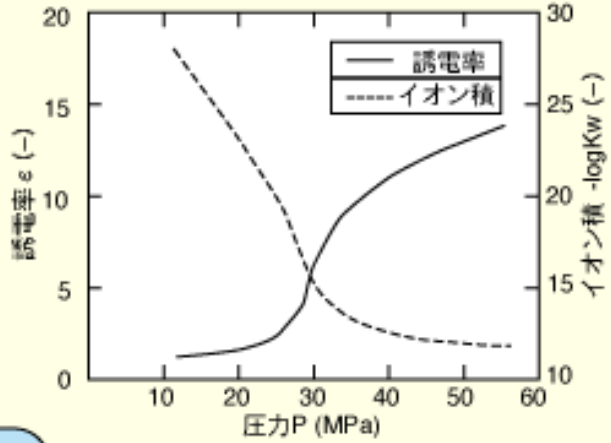

図２　超臨界水(400°C)の誘電率、
イオン積の圧力変化

Ionic product, K_w, changes depending on the solvent, temperature and pressure

⇩

Accelerate the acid-base reaction rate

⇩

Proceed the chemical reactions under mild conditions

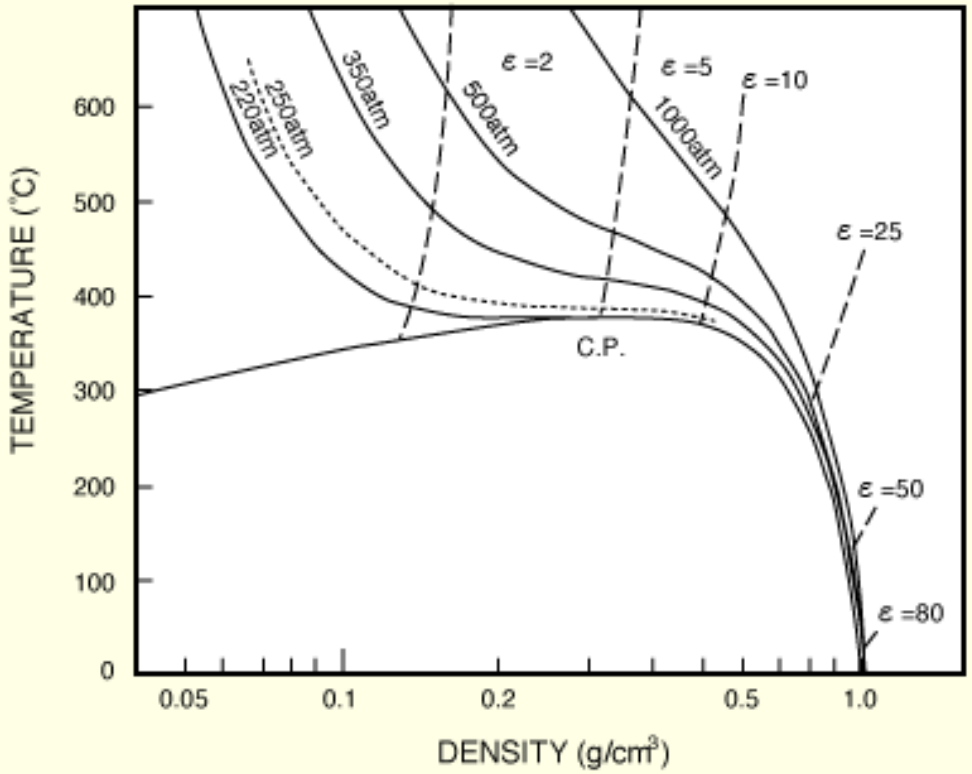

図1　高温高圧水の比誘電率の変化

(1) 圧力/温度条件により誘電率が大幅に変化

極性から無極性溶媒に対応

臨界点近傍では弱極性溶媒なみの誘電率で従来の有機溶媒に匹敵する溶解力が期待できる

有機物の比誘電率	
・プロパン	1.6
・ヘキサン	1.8
・ヘプタン	1.9
・四塩化炭素	2.2
・ベンゼン	2.3
・アセトン	20.7
・エタノール	24.5
・メタノール	32.6

Dielectric constant changes depending on the solvent, temperature and pressure

Control of the nucleation and crystal growth

Fabricate fine crystals with high crystallinity

Control of morphology, crystal growth and agglomeration using appropriate solvent and surface modifiers

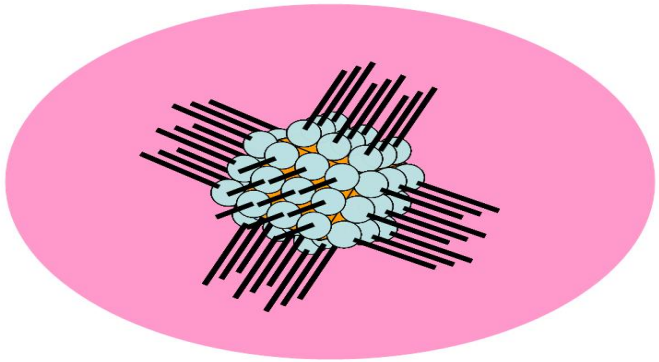

表面修飾剤の選択

硝酸Ce ＋ 直鎖C10の炭化水素
（官能基NH_2, OH, CHO, COOH）
350℃,20min（バッチ処理）

	修飾剤なし	R-OH（アルコール）	R-NH2（アミン）	R-CHO（アルデヒド）	R-COOH（カルボン酸）
結晶子径（nm）	500-1000	500-1000	50	15-20	10

カルボン酸が最も強く結合（表面修飾）する

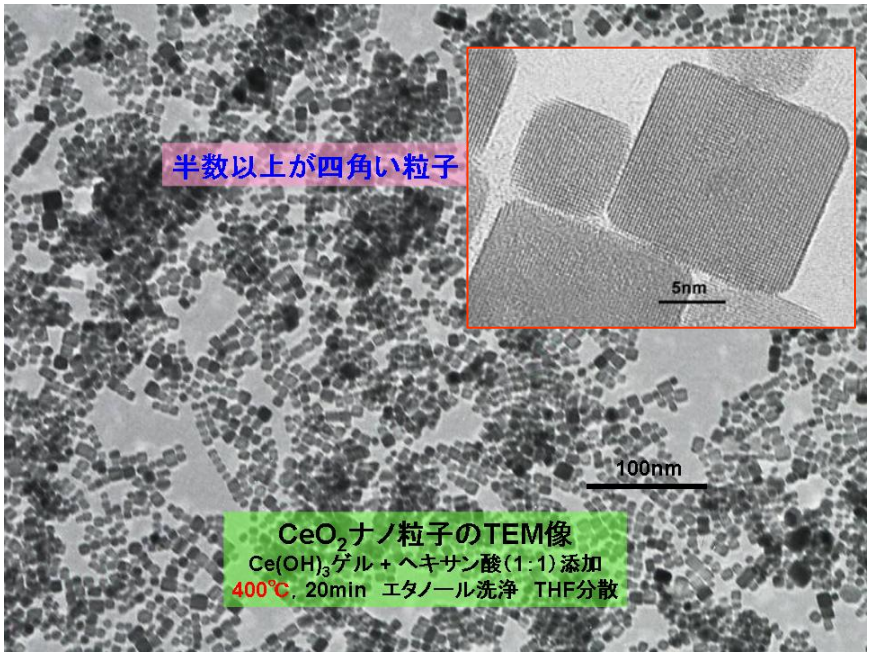

（Prof. Ajiri, IMRAM, Tohoku University）

Solvothermal reactions

Proceeding of chemical reactions under milder conditions

Depression of crystal growth and agglomeration

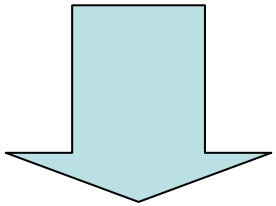

Nanocrystals with high crystallinity

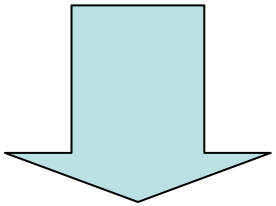

High performance photocatalyst

Solvothermal synthesis of titania photocatalysts

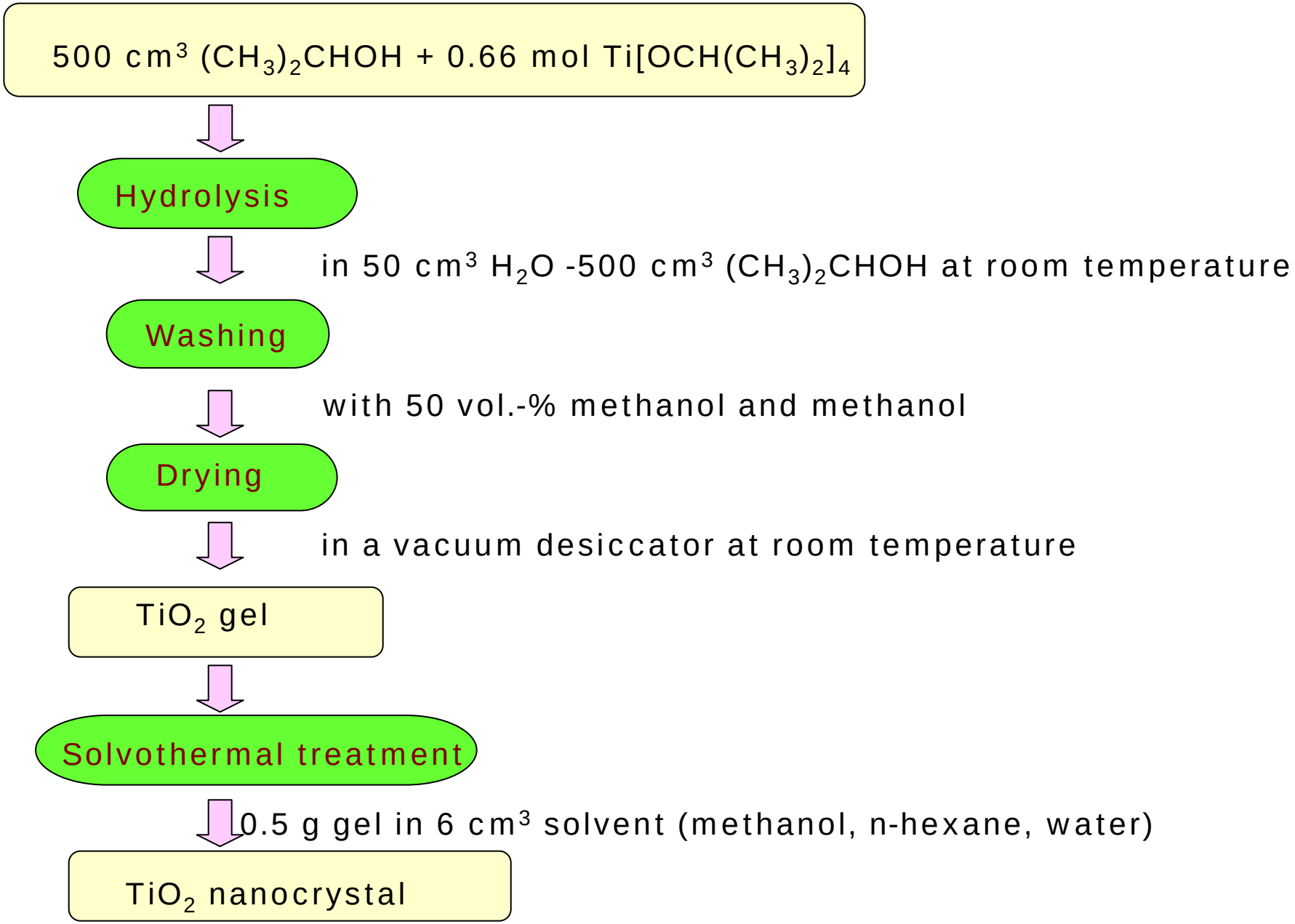

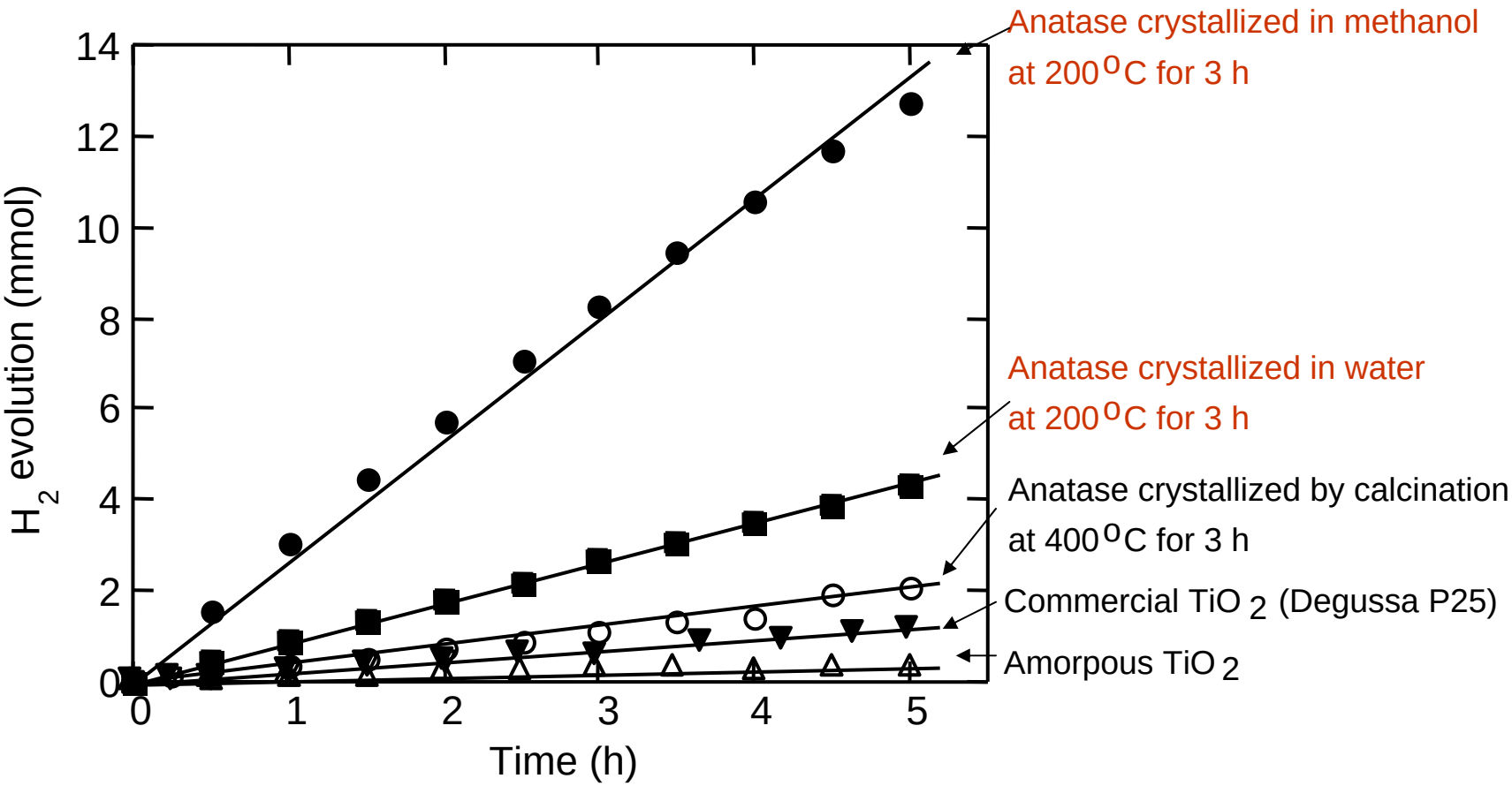

Cumulative amounts of hydrogen evolved from 0.25 g samples dispersing in 400 cm^3 50 vol% methanol solution at 60°C using 100 W high pressure mercury-arc radiation.

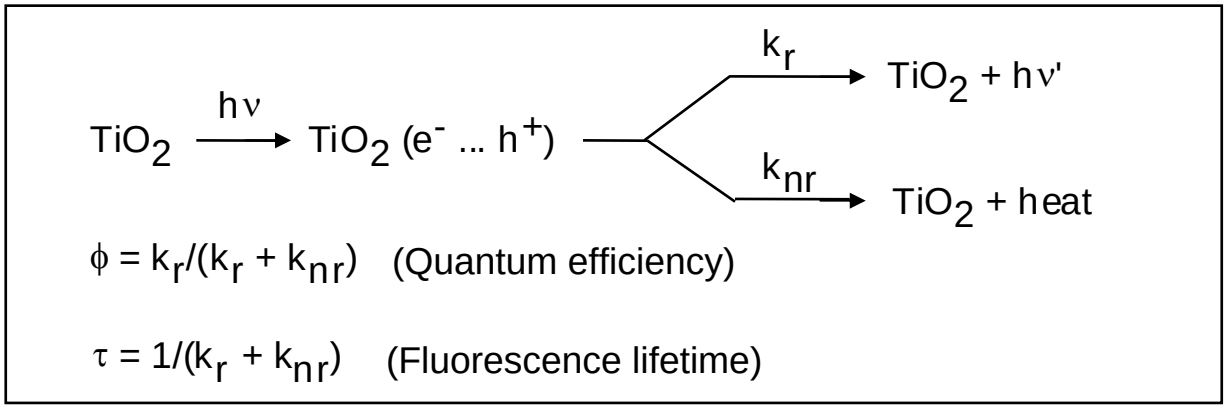

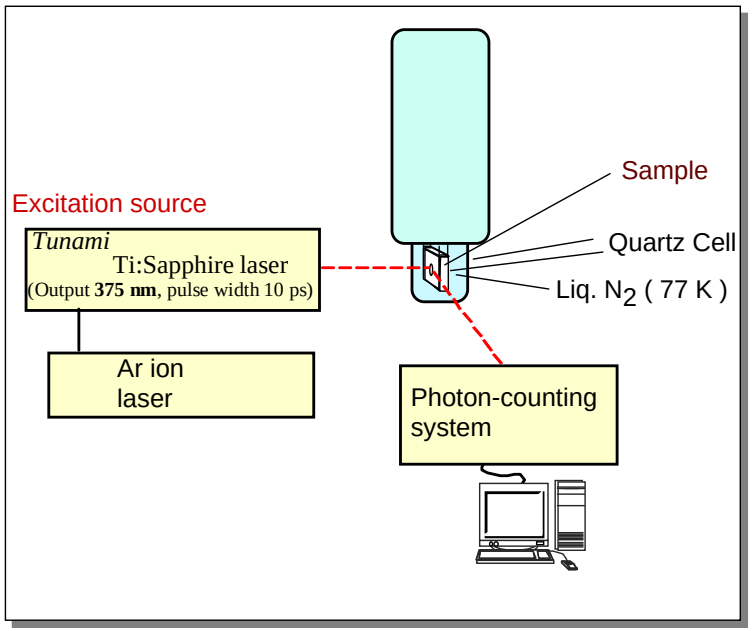

Time-resolved emission spectra measurements

(URAS in Tohoku Univ.)

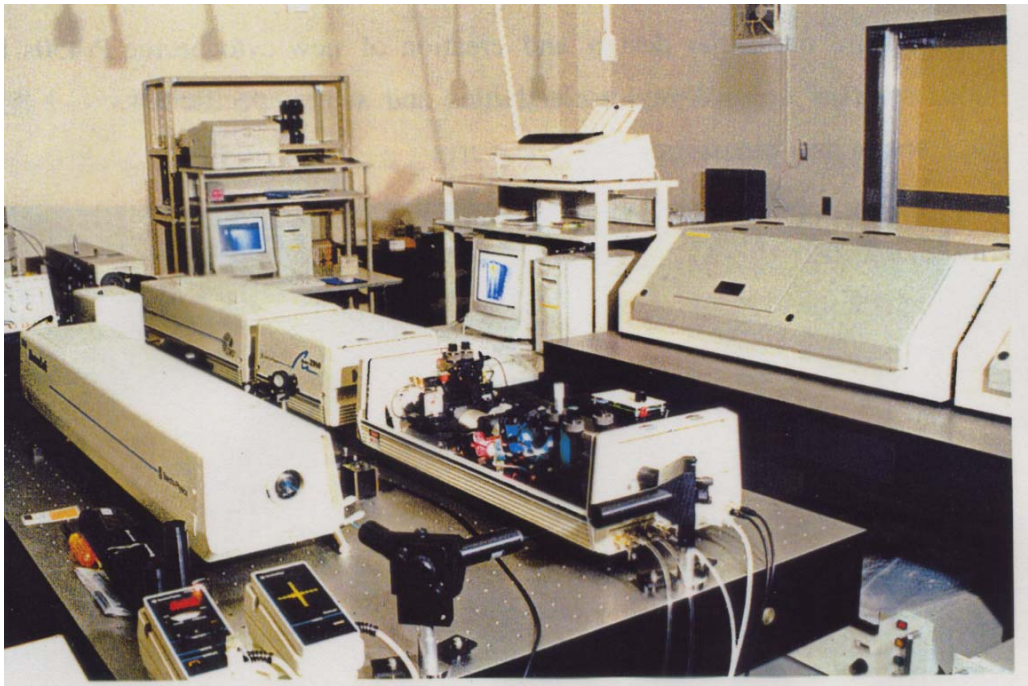

Laser flash photolysis system with pico-second time resolution

ピコ秒の時間分解能をもつレーザー・フラッシュ・ホトリシス装置

Solvothermal synthesis → Fine crystals, High crystallinity → Excellent photocatalytic activity

S. Yin, Y. Inoue, S. Uchida, Y. Fujishiro, T. Sato, *J. Mater. Res.*, 13, 844 (1998).

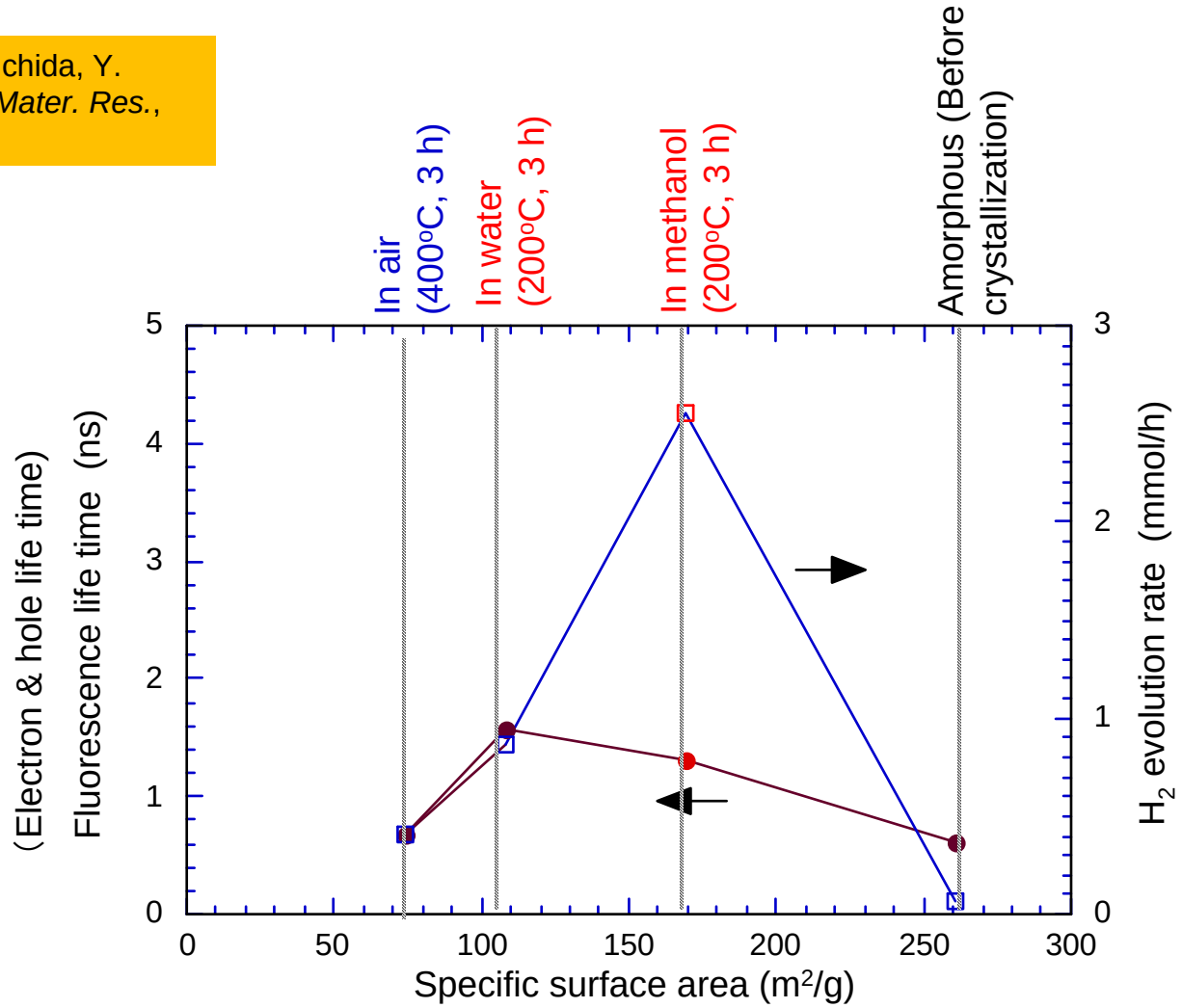

Photocatalytic activity of titania crystallized under various conditions

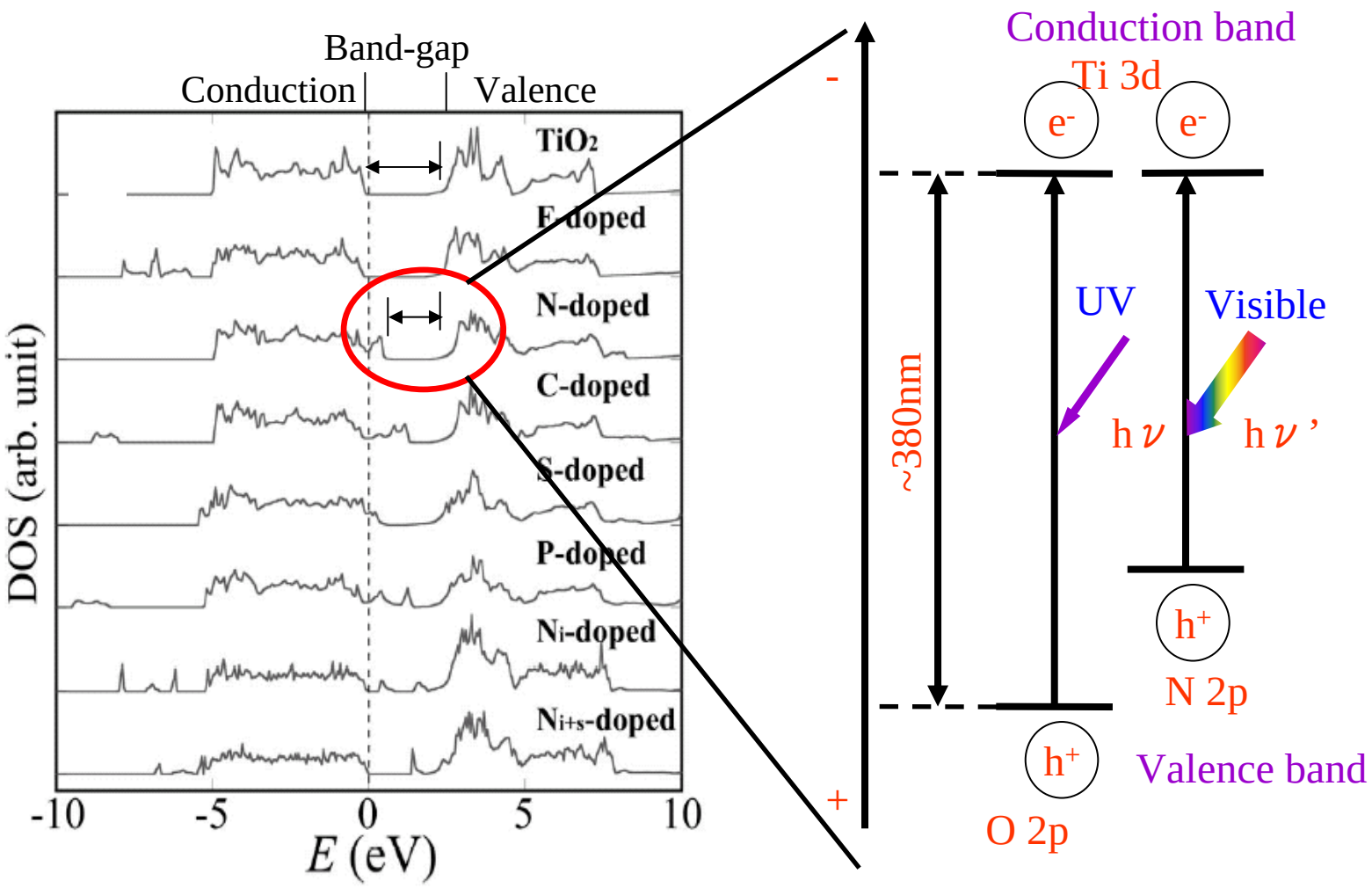

Total DOSs of doped TiO_2 calculated by FLAPW

Schematic illustration of visible light response by nitrogen doping

Ref. R.Asahi et al., *Science*, 293, 269 (2001)

Preparation of nitrogen-doped titania

Solid-gas reaction: Calcining titania in nitrogen and/or ammonia gas atmosphere at 550-600°C

R. Asahi, T. Morikawa, T. Ohwaki, A. Aoki, and Y. Taga: Science, 293, 269 (2001).

Solid-liquid reaction: Treating amorphous hydrous titania with ammonia solution followed by calcination around 400°C

S. Sato: Chem. Phys. Lett., 123, 126 (1986).

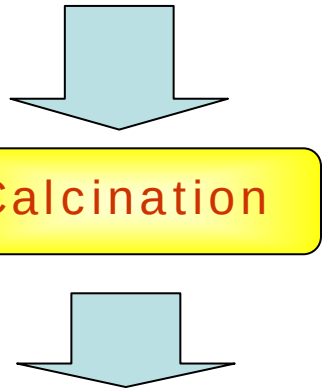

Decrease the nitrogen content

Decrease the specific surface area

Decrease the photocatalytic activity

Preparation of nitrogen ion-doped titania nanoparticles by the solvothermal reactions : liquid phase reaction without calcination

Hexamethylenetetramine-
0.38 M $TiCl_3$ mixed aq. solution

↓

Heat at 90°C for 1 h

↓

Heat at 110-230°C for 1 h

↓

Centrifuge

↓

Wash

↓

Vacuum dry at 60°C overnight

Homogeneous precipitation

$C_6H_{12}N_4 + 6\ H_2O \rightarrow 6HCHO + 4NH_3$

$TiCl_3 \rightarrow TiO_{2-1.5x}N_x \cdot nH_2O$

Crystallization

$TiO_{2-1.5x}N_x \cdot nH_2O \rightarrow TiO_{2-1.5x}N_x + nH_2O$

$C_6H_{12}N_4$ added (M)	Final pH
0.29	1
0.86	7
1.43	9

Compounds used as nitrogen sources

Hexamethylenetetramine (HMT)

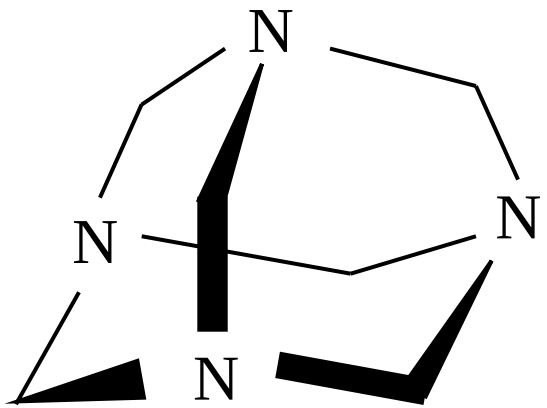

Urea

NH_2-CO-NH_2

Monoethanol amine(MEA)

$H_2N-CH_2CH_2OH$

Diethanol amine(DEA)

$HN(CH_2CH_2OH)_2$

Triethanol amine(TEA)

$N(CH_2CH_2OH)_3$

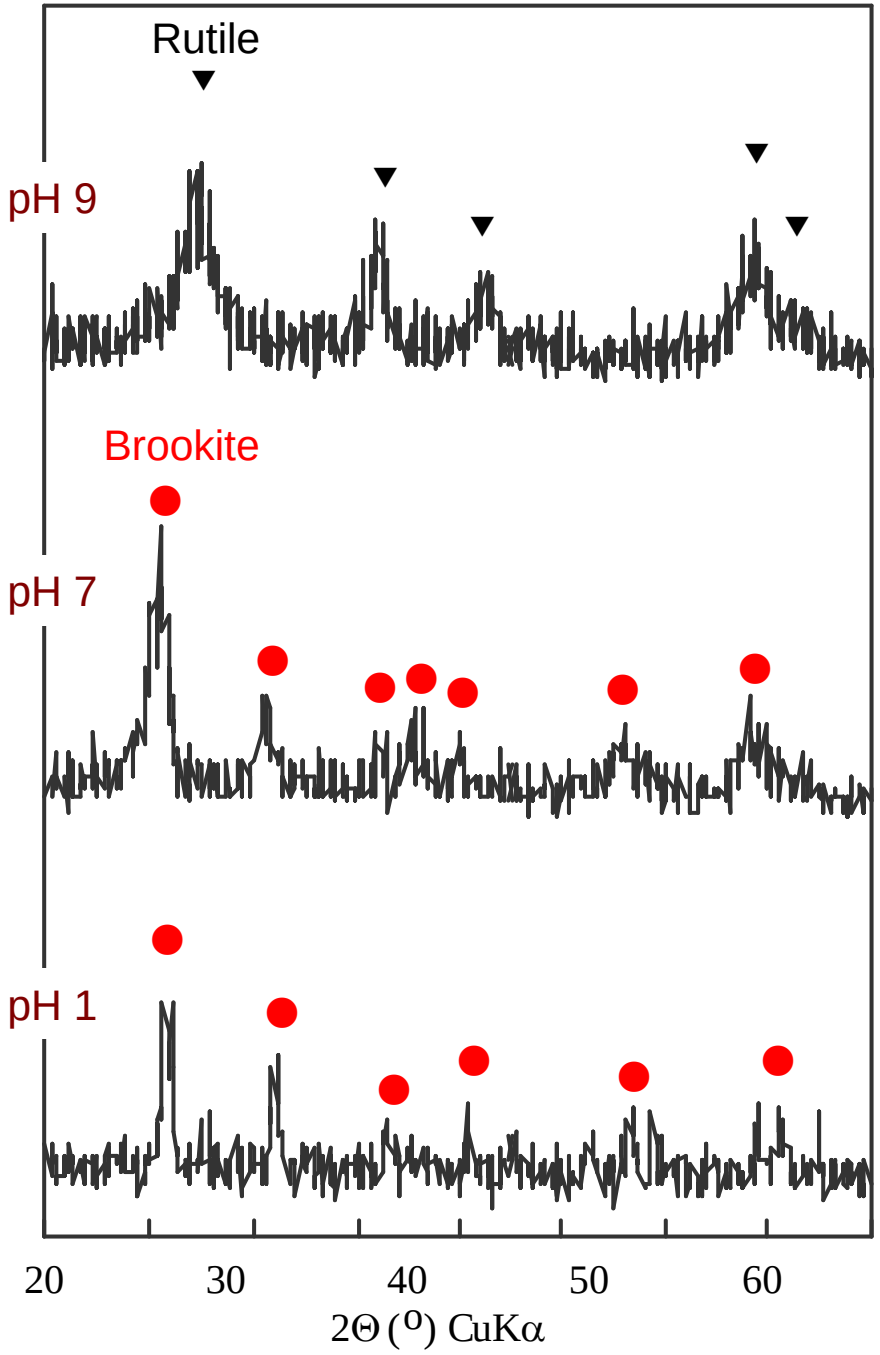

TiO_2 (Degussa P25)

Product at pH 7

Product
pH 1-7: Brookite
pH 9 : Rutile

$C_6H_{12}N_4 + 6\ H_2O \rightarrow 6HCHO + 4NH_3$

XRD patterns of the powders prepared by the homogeneous precipitation-solvothermal process in $TiCl_3$-hexamethylenetetramine aqueous solutions at 190°C and final pH (a) 1, (b) 7 and (c) 9 for 2 h.

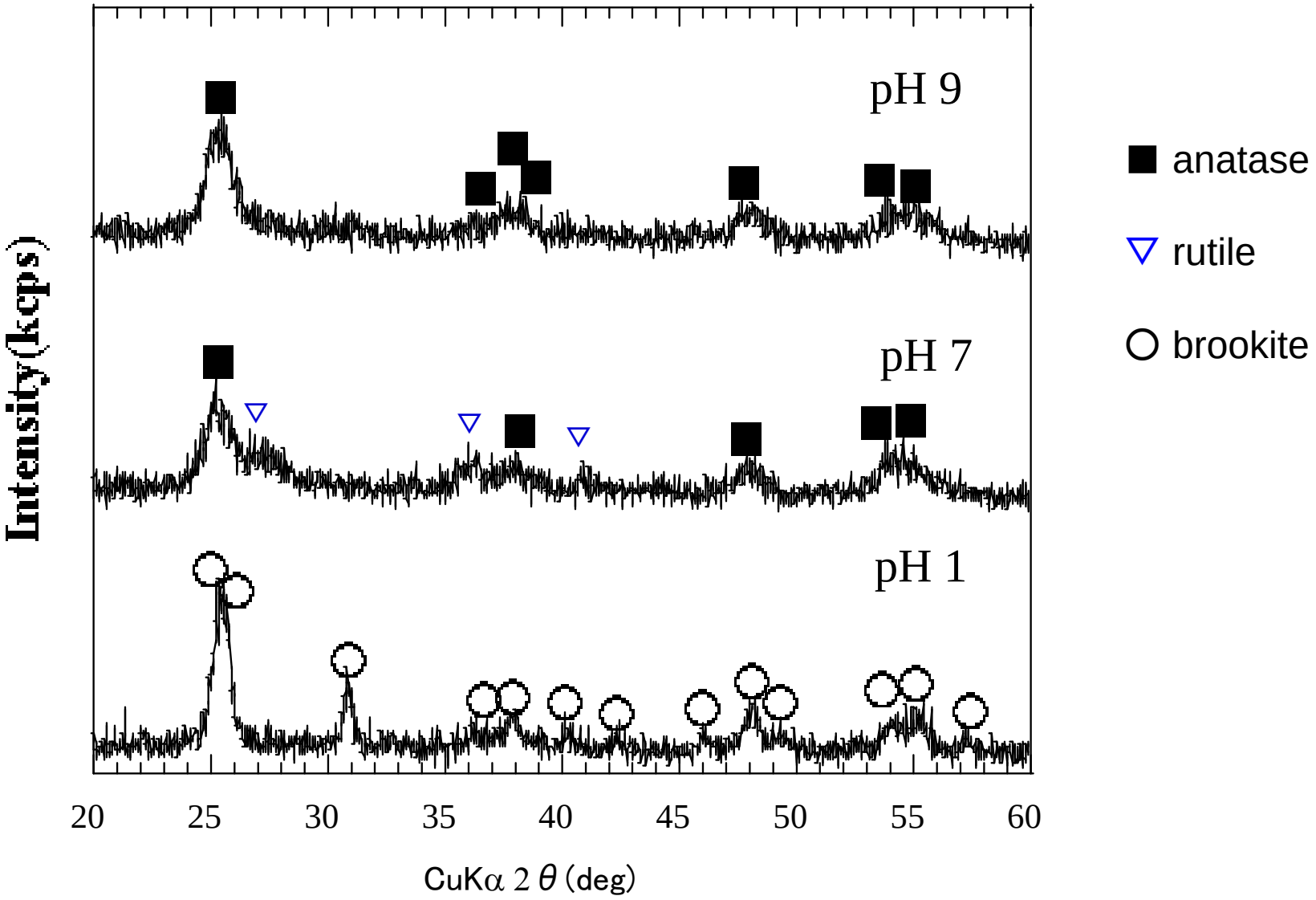

XRD patterns of nitrogen doped TiO_2 powders prepared in $TiCl_3$-hexamethylenetetramine-methanol aqueous solution.

Formation of single phases of anatase, rutile & brookite type $TiO_{2-x}N_y$

S.Yin et . al., *J. Mater. Chem.*,15, 674-682, (2005)

Raman

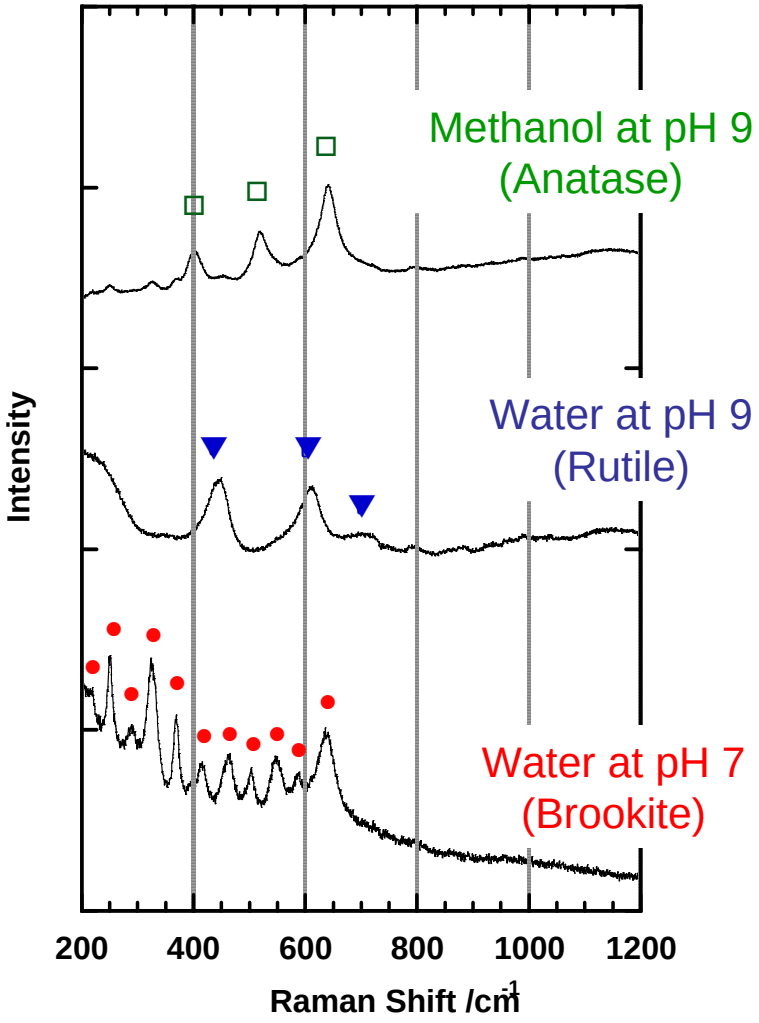

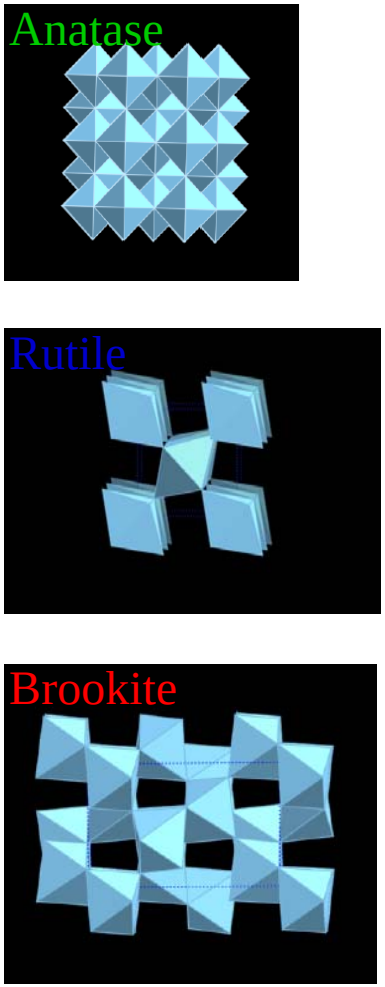

XPS

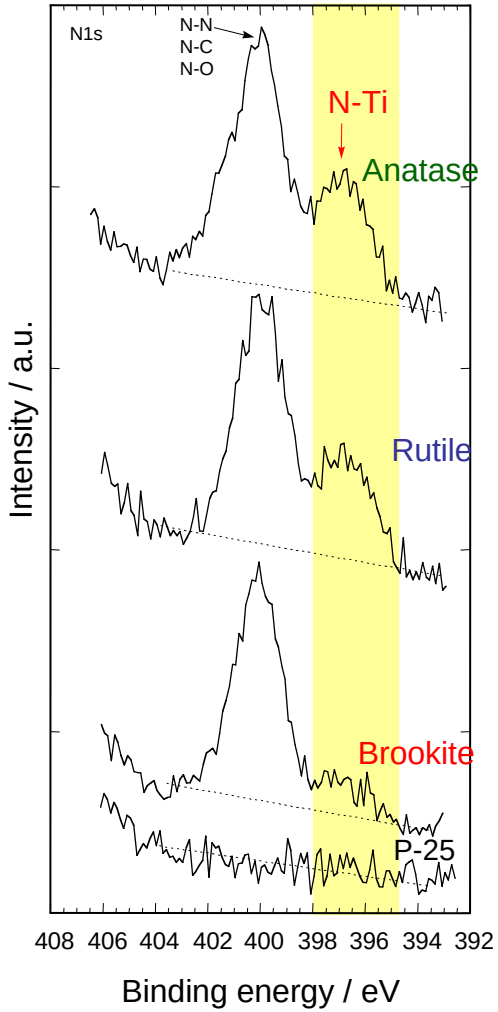

Raman and XPS spectra of nitrogen-doped titania prepared by solvothermal reactions under various conditions

Effect of pH value & solvents

S. Yin, etc., J. Mater. Chem., 15, 674 (2005).

$TiCl_3$ - HMT - water

$TiCl_3$- HMT- methanol

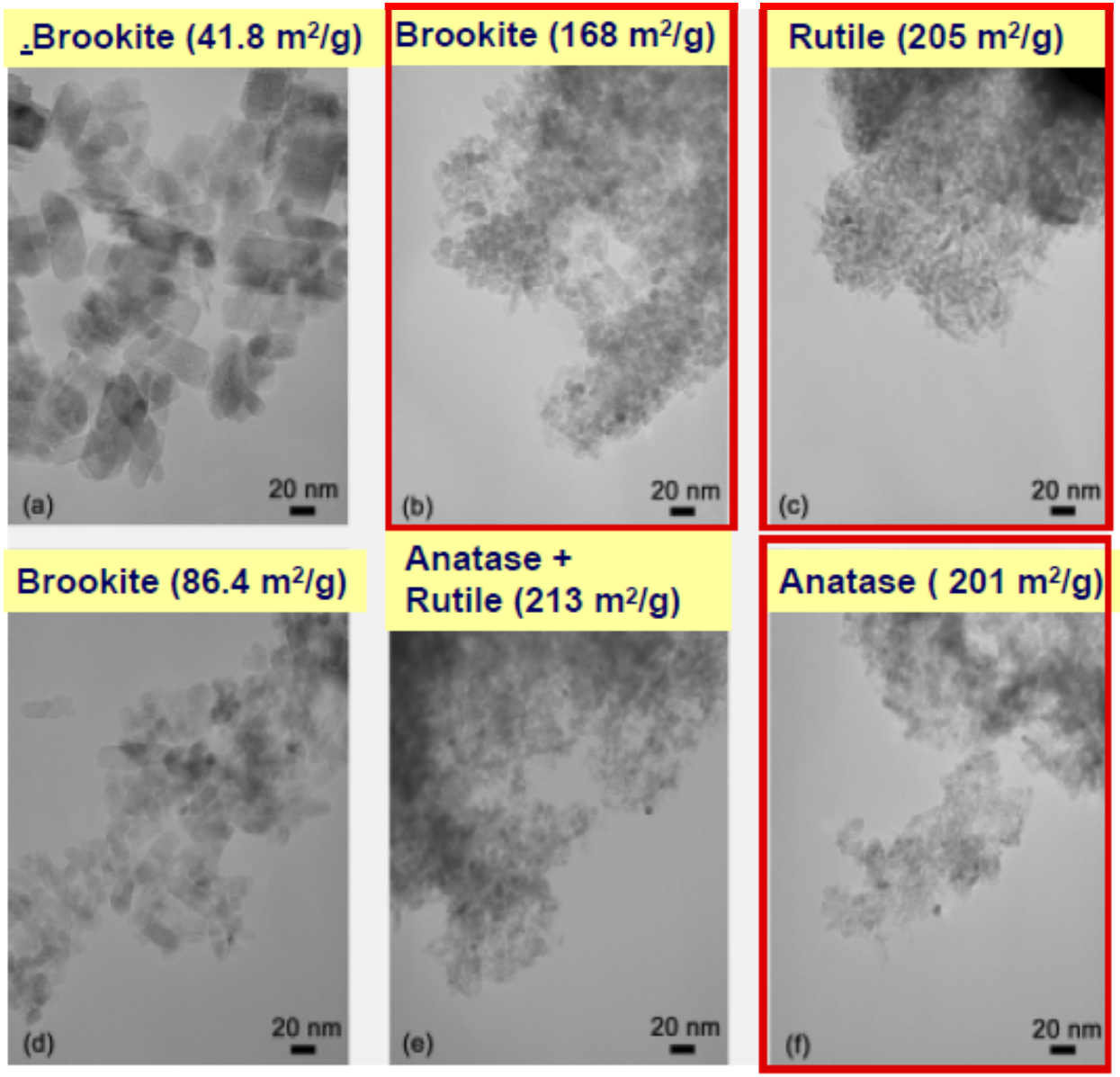

TEM photographs of the powders prepared in $TiCl_3$-HMT aqueous solutions and $TiCl_3$-HMT methanol solution at pH 1, 7 and pH 9 and 190°C for 2 h.

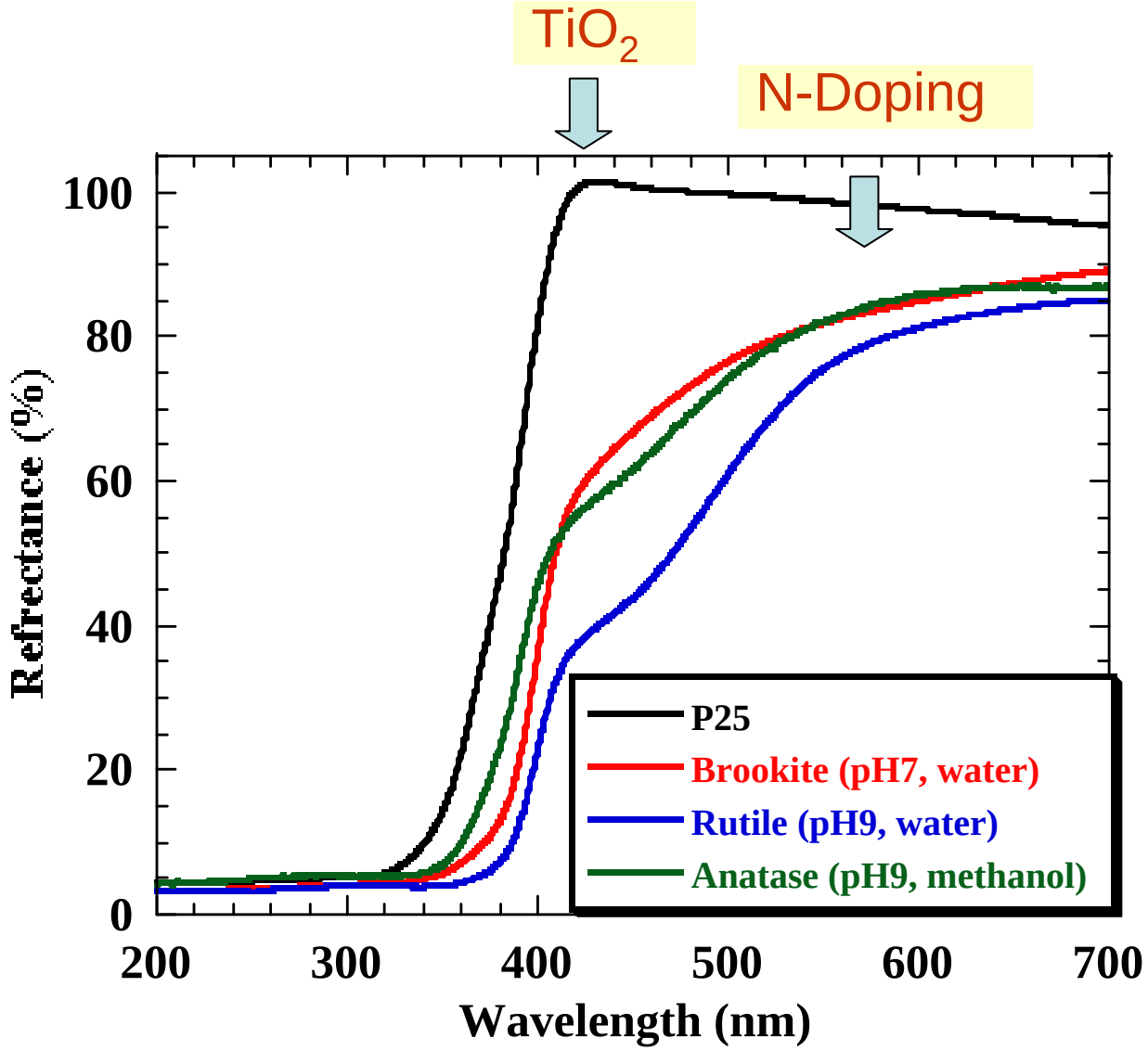

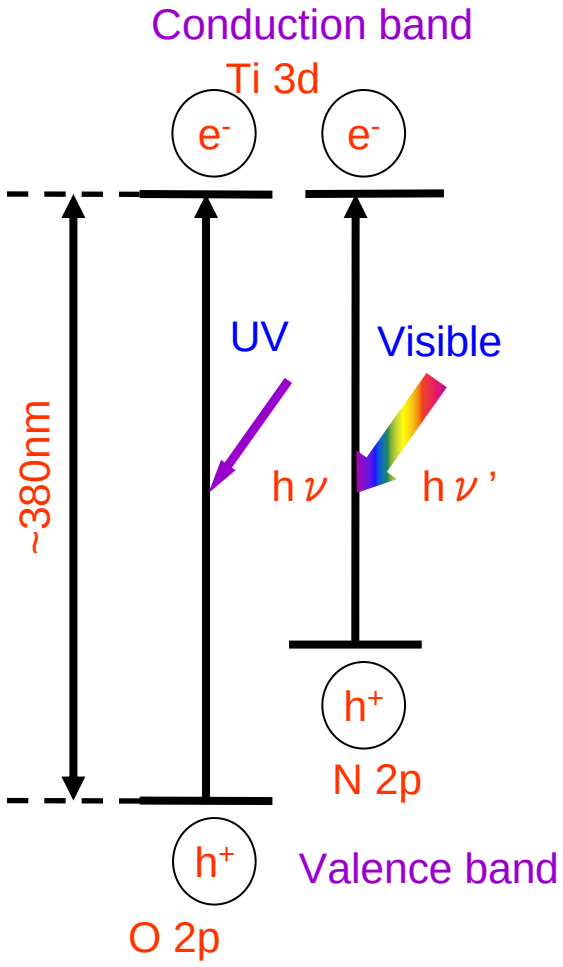

Diffuse reflectance spectra of titania powders prepared by solvothermal reactions followed by calcination in air at 400°C for 1h

Photocatalytic reaction apparatus for the oxidative decomposition of nitrogen monoxide

Reactor volume: 373 cm^3
Flow gas: 1 ppm NO
Flow rate: 200cm^3/min
Residence time: 1.87 min
Catalyst: 20 × 16 × 0.5 mm^3
Light: 450 W high pressure Hg lamp

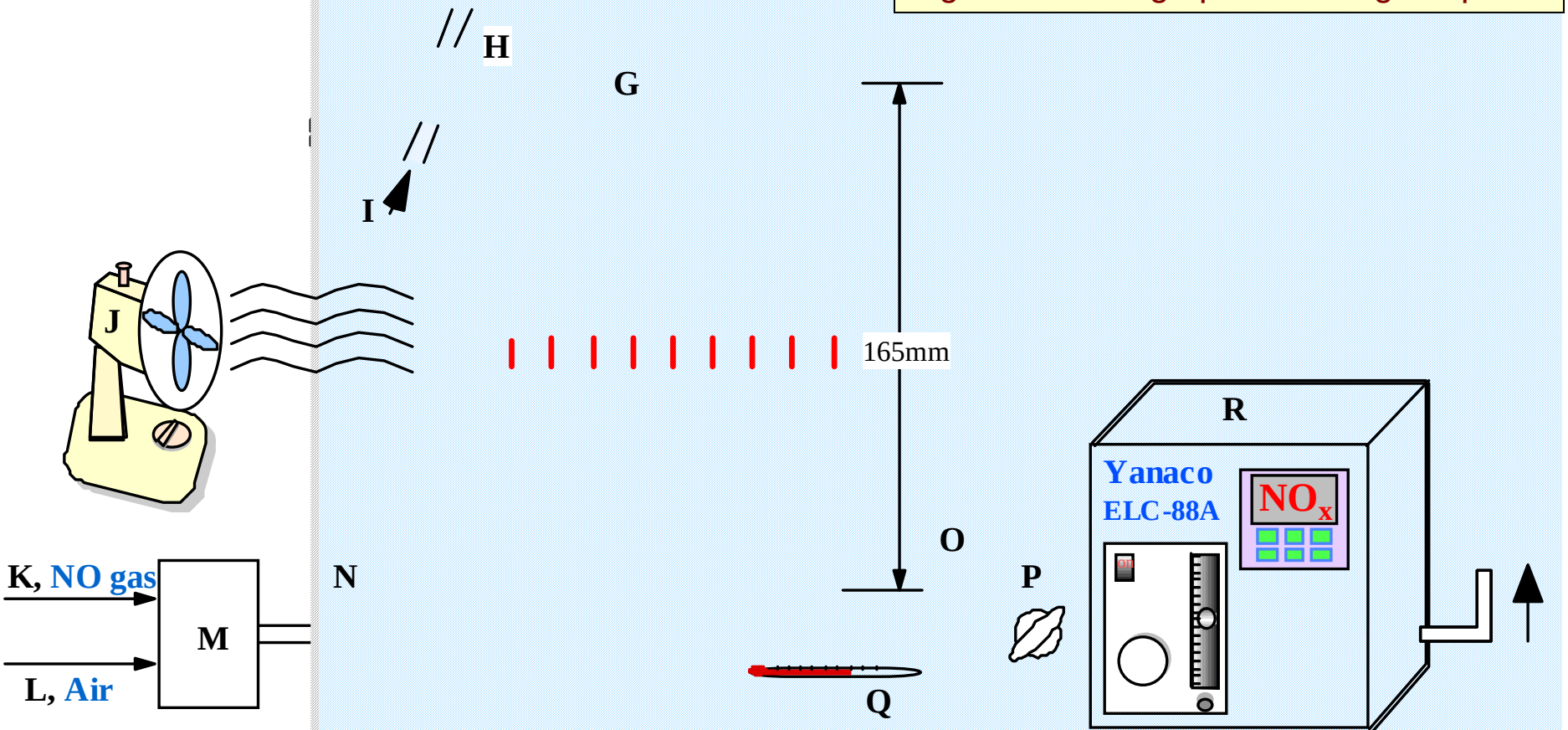

$NO + 3/4\ O_2 + 1/2\ H_2O \rightarrow HNO_3$

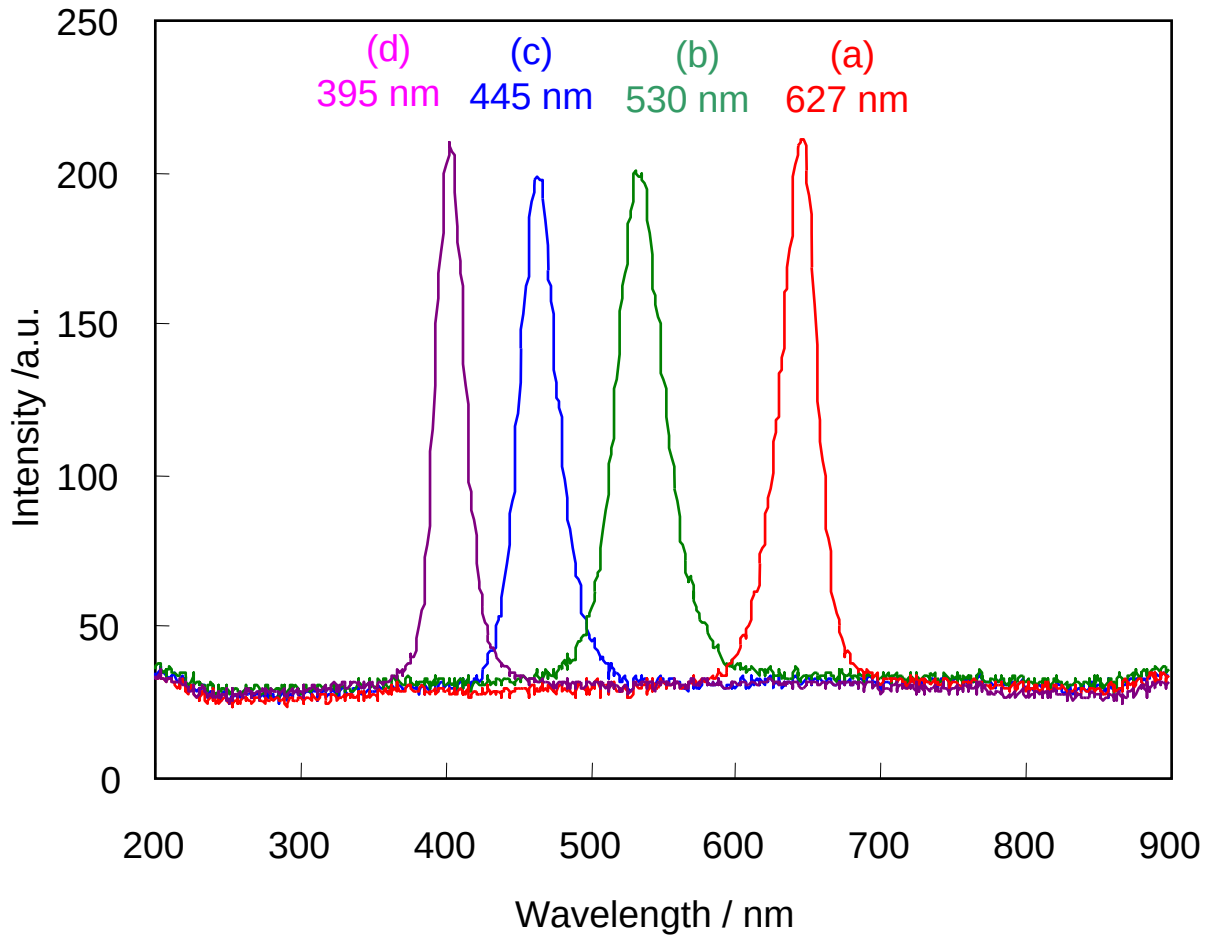

Wavelength distributions of LED light used

(a) Red light LED (627 nm)

(b) Green light LED (530 nm)

(c) Blue light LED (445 nm

(d) UV light LED (395 nm)

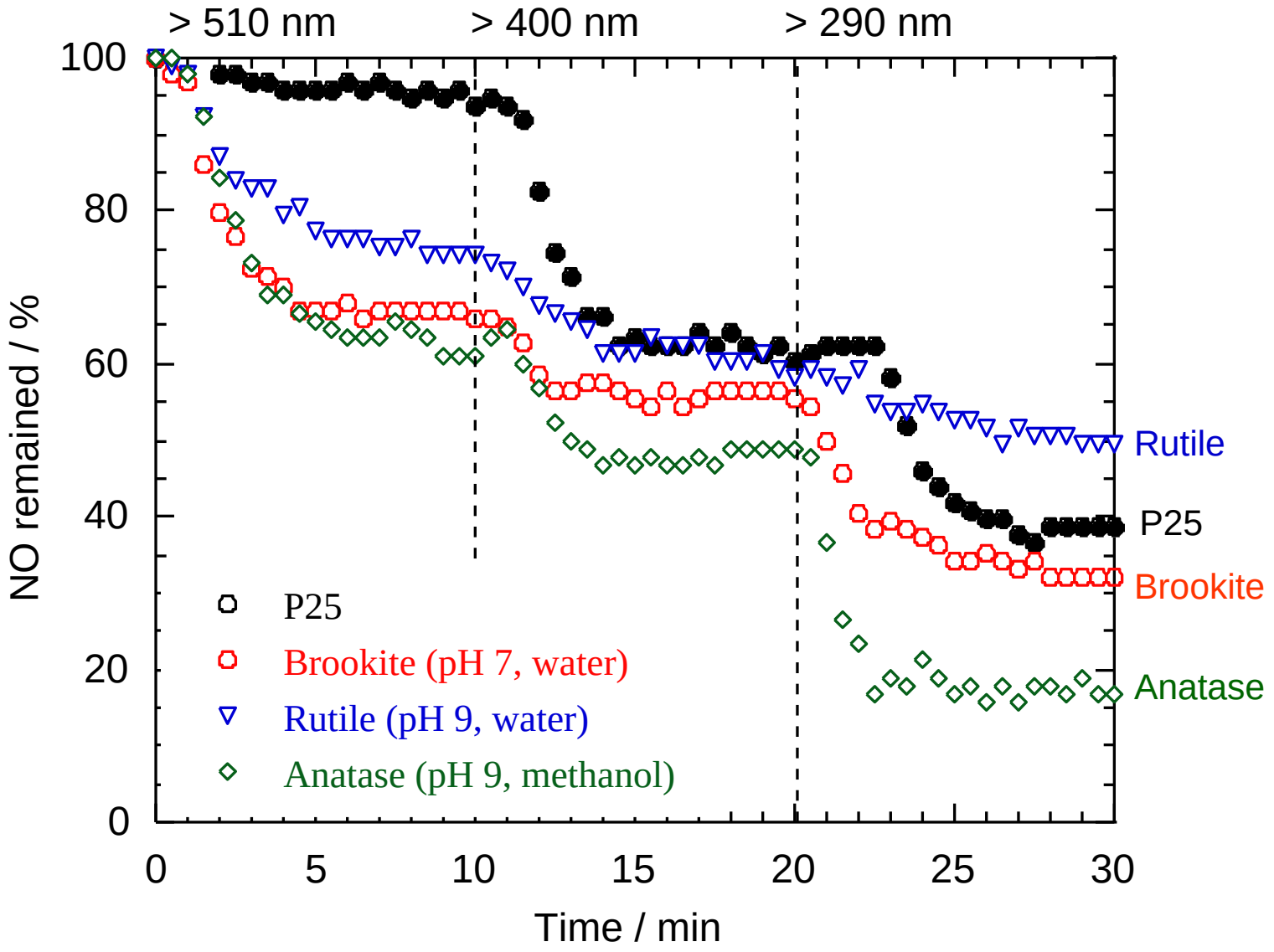

Photocatalytic activities of different crystalline phases of nitrogen-doped titania for the oxidative decomposition of NO

Phtocatalytic activity: Anatase > Brookite > Rutile

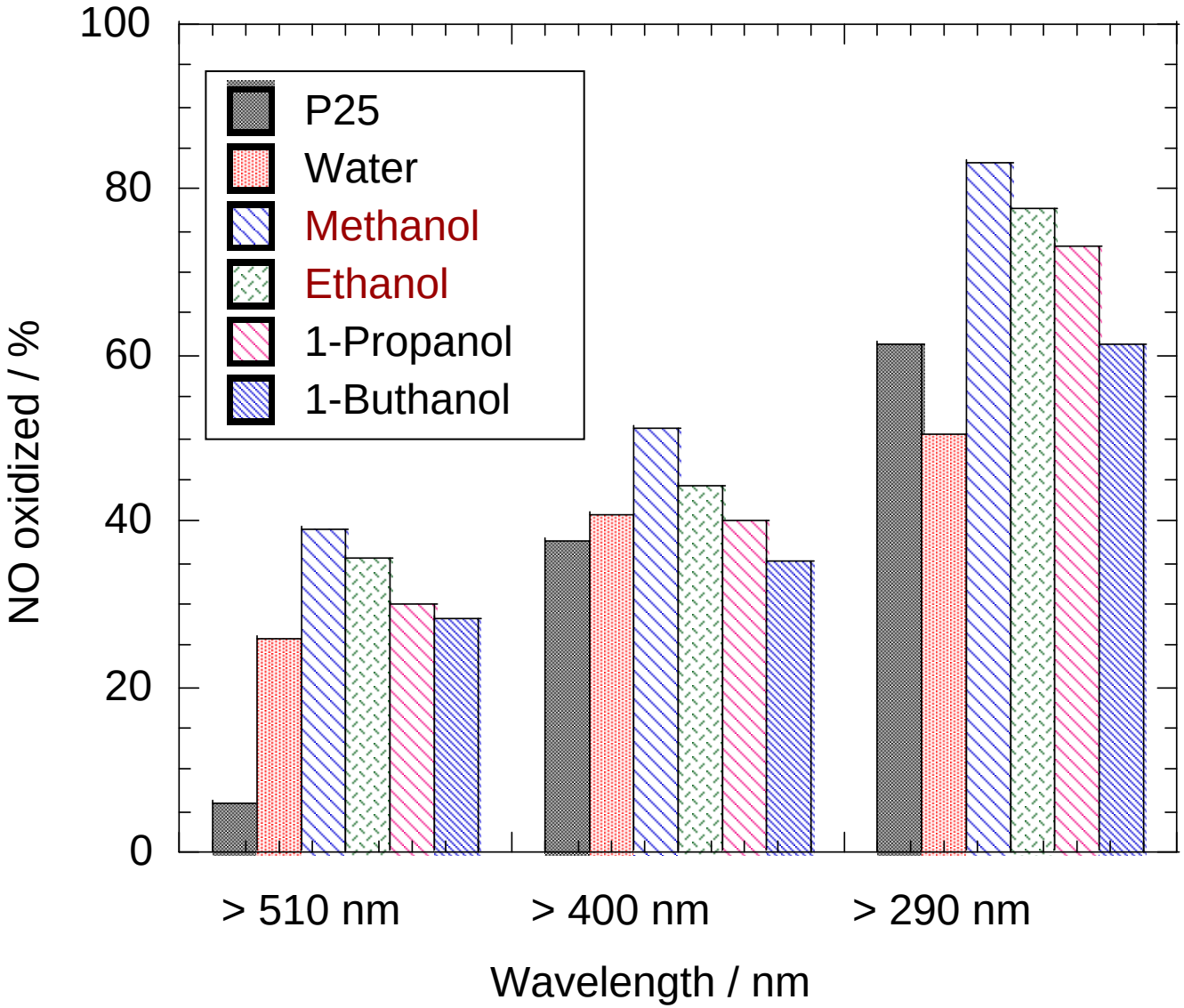

Photocatalytic activity of nitrogen doped titania prepared in various solvents for the oxidative decomposition of nitrogen monoxide under irradiating 450 W high pressure mercury arc filtered with various cut filters. Initial NO concentration: 1 ppm.

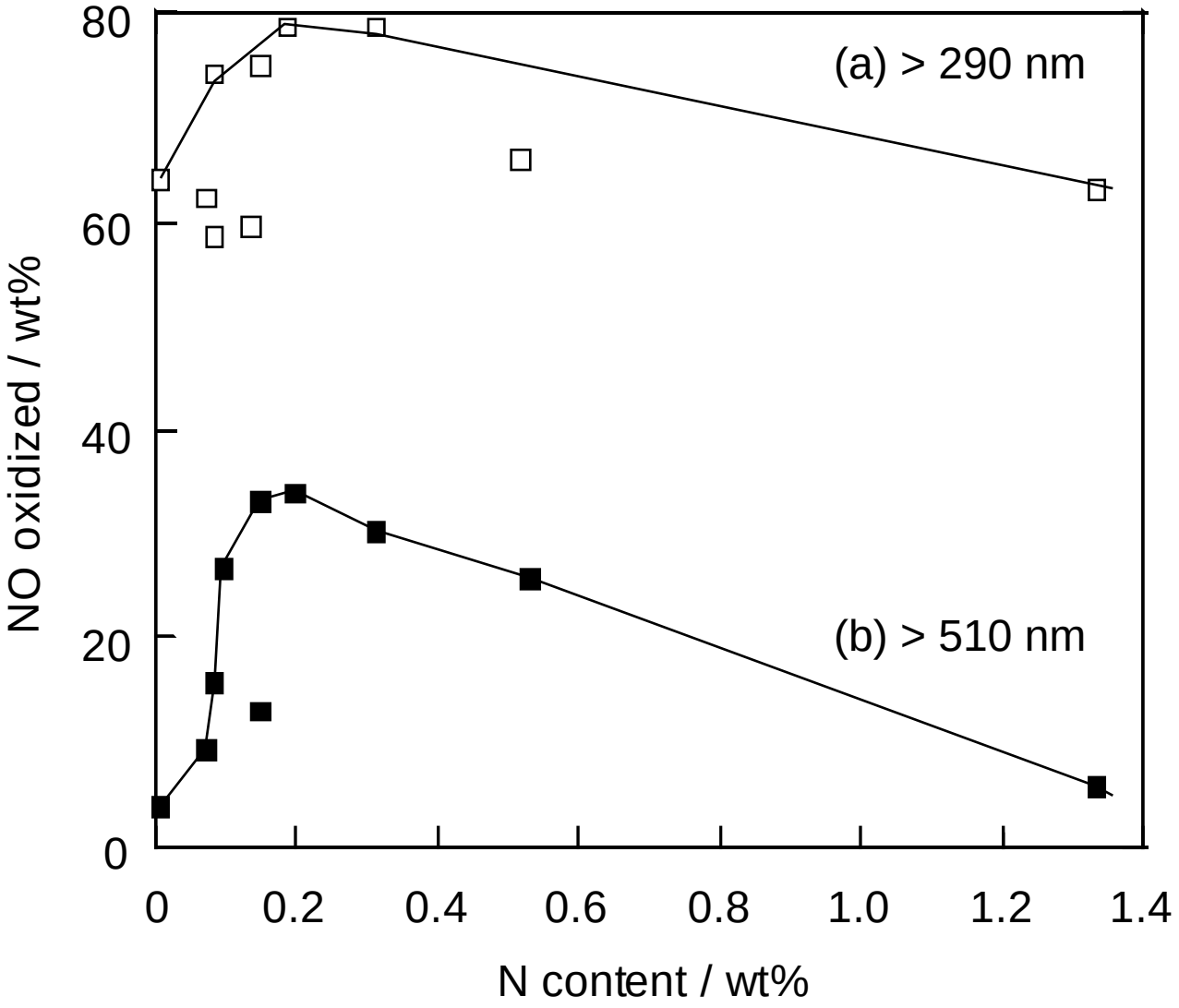

Relationship between the nitrogen content and photocatalytic activity of nitrogen doped titania prepared in various solvothermal conditions. Initital NO concentration: 1 ppm, Irradiation light: 450 W high pressure mercury arc filtered with (a) 290 and (b) 510 nm cut filters.

Anion defect in Nitrogen doped TiO_2

$Ti(O^{2-})_{2x}(N^{3-})_x\square_{x/2}$

Positive effect: Increase the visible light absorption ability

Negative effect: Formation of anion defect which becomes the electron-hole recombination center

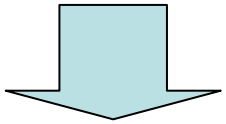

Optimum nitrogen doping content

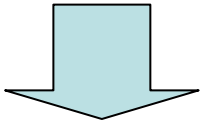

Improve the photocatalytic performance

Decrease the lattice defect

Improvement of photocatalytic activity by decreasing the lattice defect

- Co-doping of nitrogen ion and higher valence metal ion

  $(Ti^{4+}_{1-x}Nb^{5+}_{x})(O^{2-}_{2-x}N^{3-}_{x})$

- Co-doping of nitrogen ion and lower valence anion

  $Ti(O^{2-}_{2x}N^{3+}_{x}F^{-}_{x})$

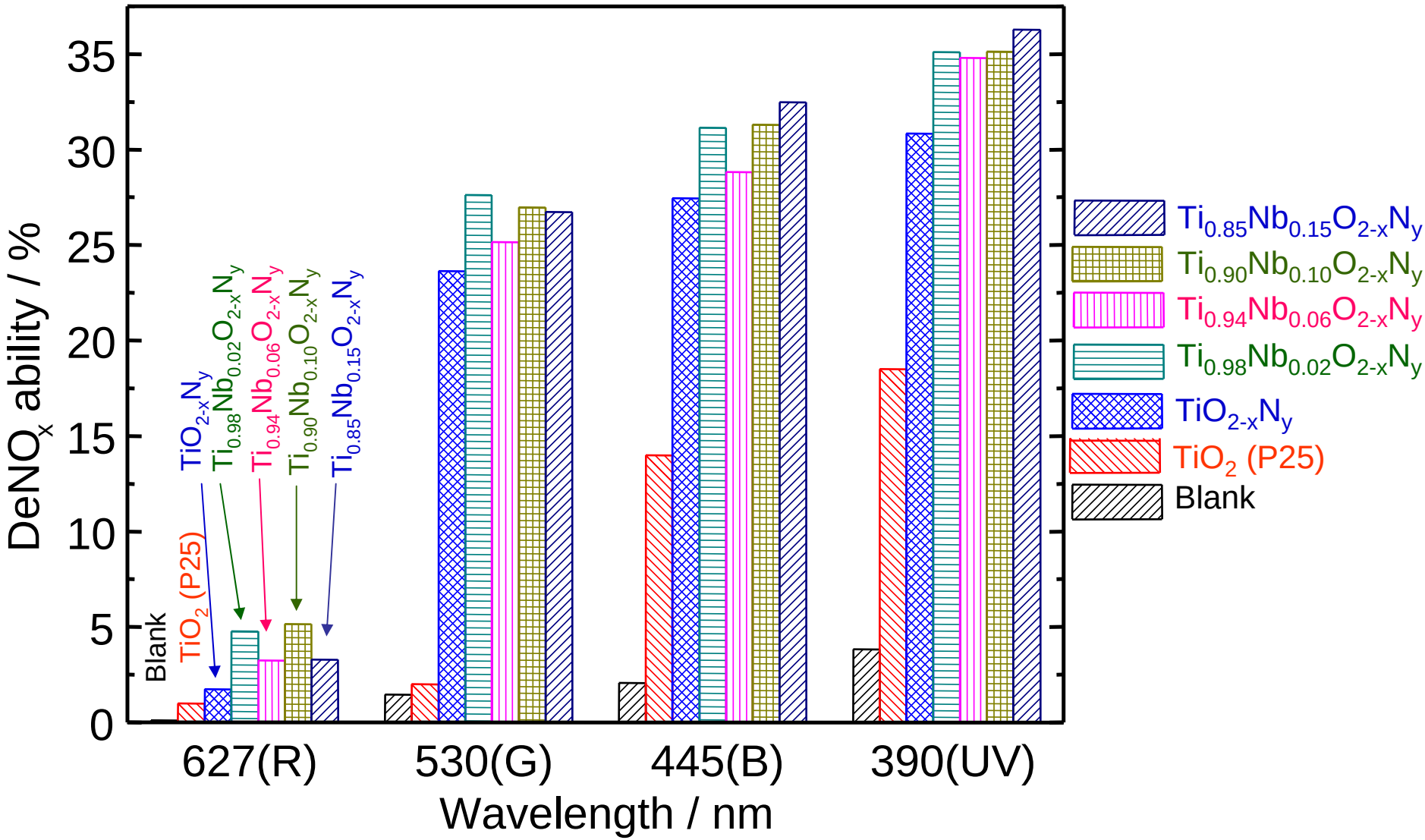

Photocatalytic activity in deNO$_x$ by (a) blank (no catalyst), (b) undoped TiO_2 (Degussa P25), (c) $TiO_{2-x}N_y$ and $TiO_{2-x}N_y$ co-doped with (d) 2 mol.%, (e) 6 mol.%, (f) 10 mol.%, and (g) 15 mol.% of Nb

Improvement of photocatalytic activity by depressing the electron-hole recombination with heterogeneouos electron transfer

Composites with semiconductors possessing different band structures

$TiO_{2-x}N_y/TiO_2$

$TiO_{2-x}N_y/Fe_2O_3$

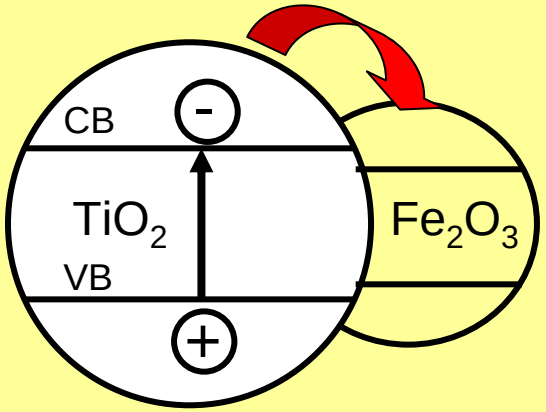

Composites with metals

$TiO_{2-x}N_y/Pt$

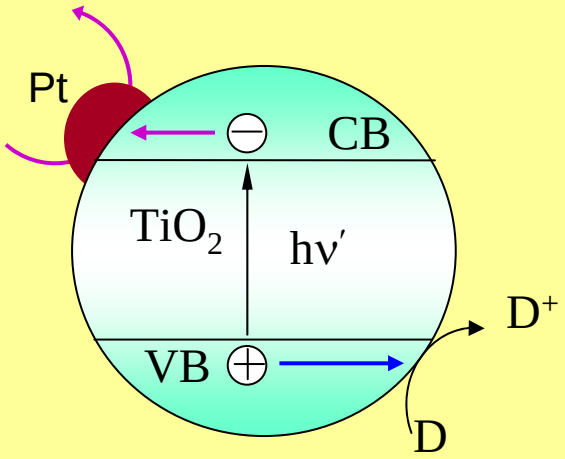

Photocatalytic deNO$_x$ abilities evaluated by irradiating different LED lights

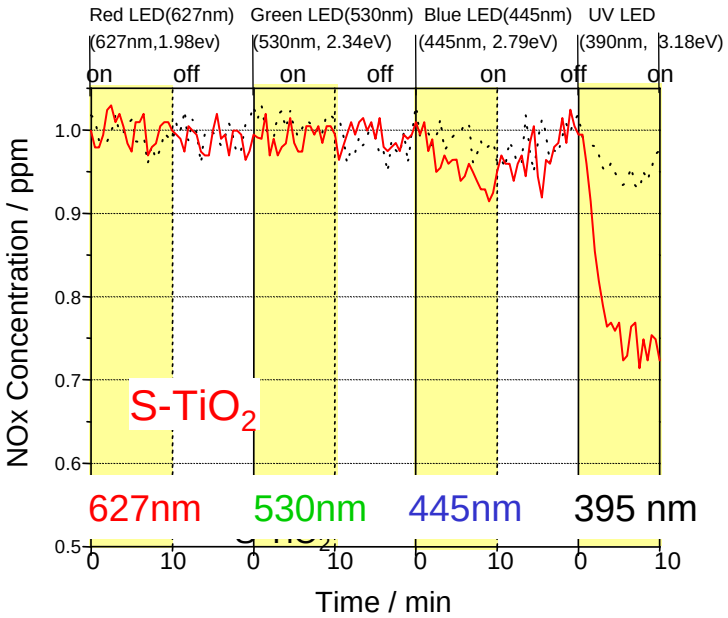

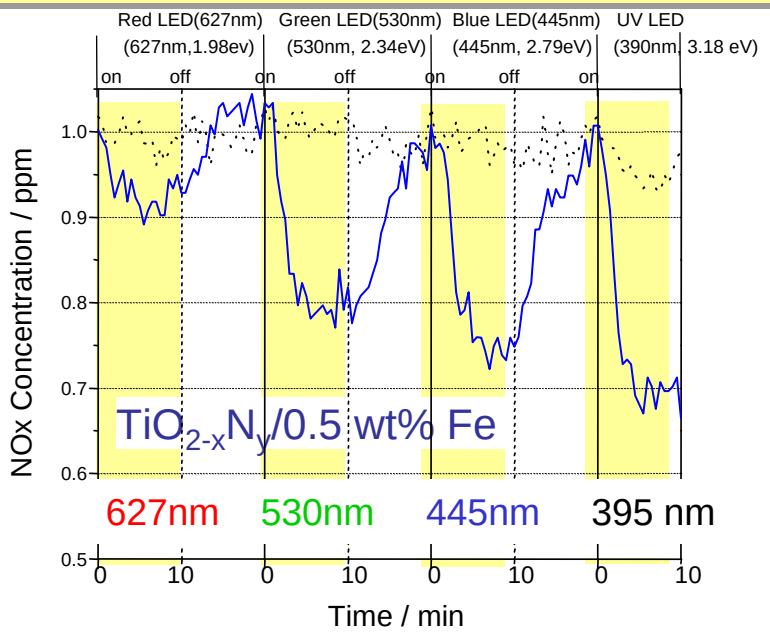

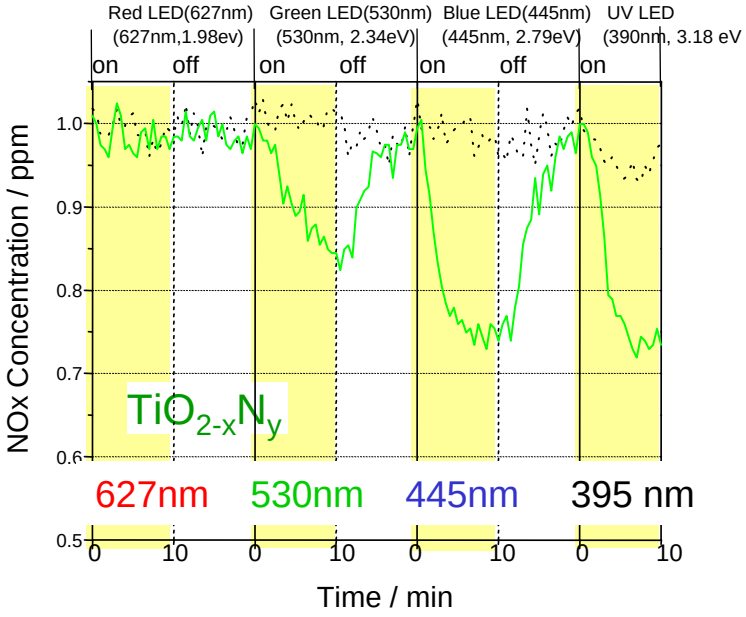

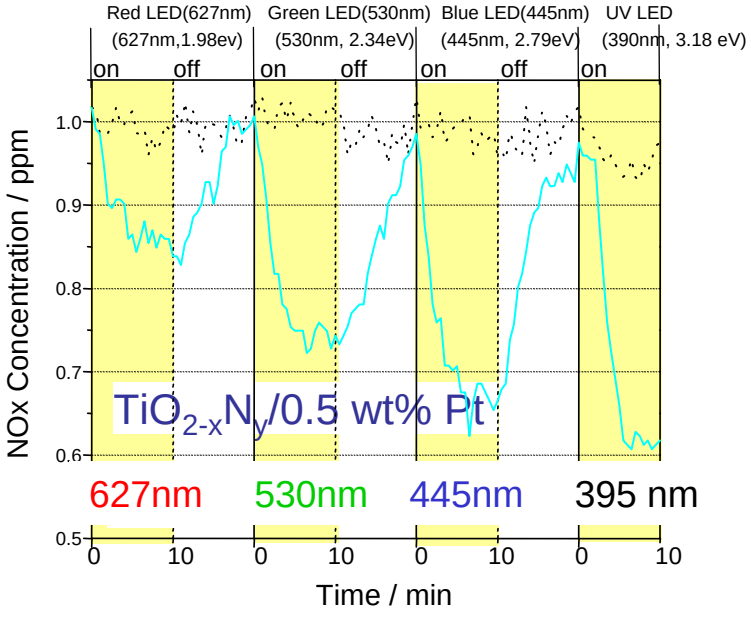

Reactor volume： 370 cm^3、Gas flow rate：200 cm^3/min、NO conc.：1 ppm Light soource：LED lamp (2mW/m^2)

Composite with Attapulgite

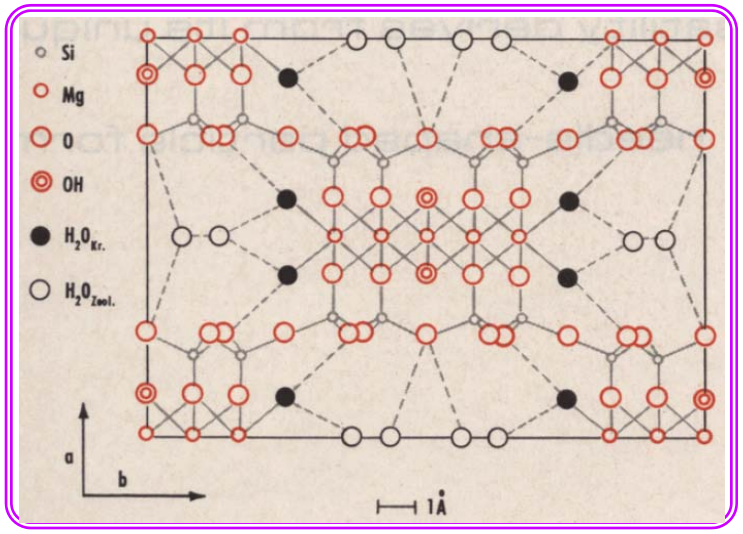

A natural mineral

$Mg_5(Si,Al)_8O_{20}(OH)_2 \cdot 8H_2O$

Applications:

Constructing materials, Decolorizing agents, etc.

$TiO_{2-x}N_y$/Attapulgite

Photocatalytic activity

Adsorption ability

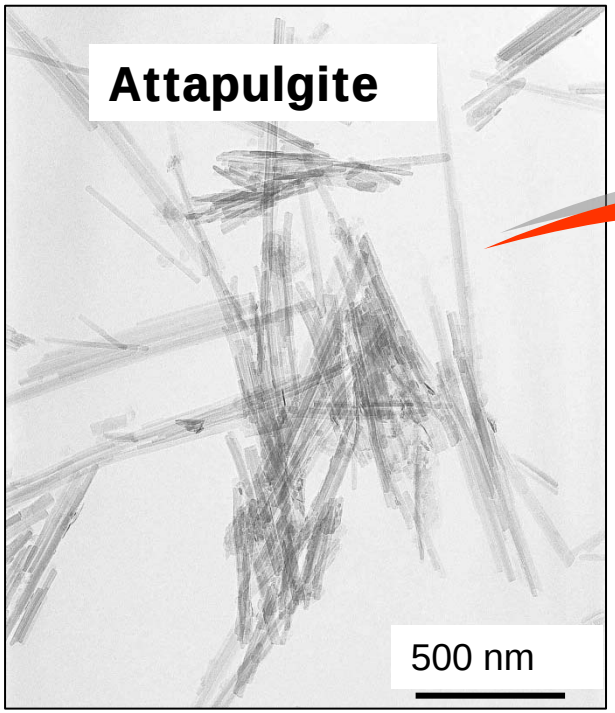

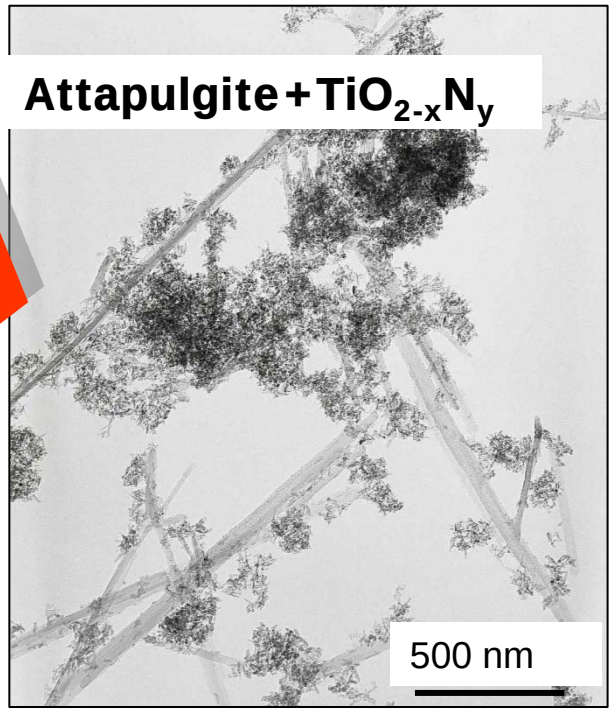

Sample	Attapulgite	$TiO_{2-x}N_y$	$TiO_{2-x}N_y$ /Attapulgite
Pore size (dV(d)) / nm	3.83	12.36	12.38
Pore volume / cm^3/g	0.33	0.49	0.79
Specific surface area / m^2/g	211	202	213

Influence of $TiO_{2-x}N_y$ content

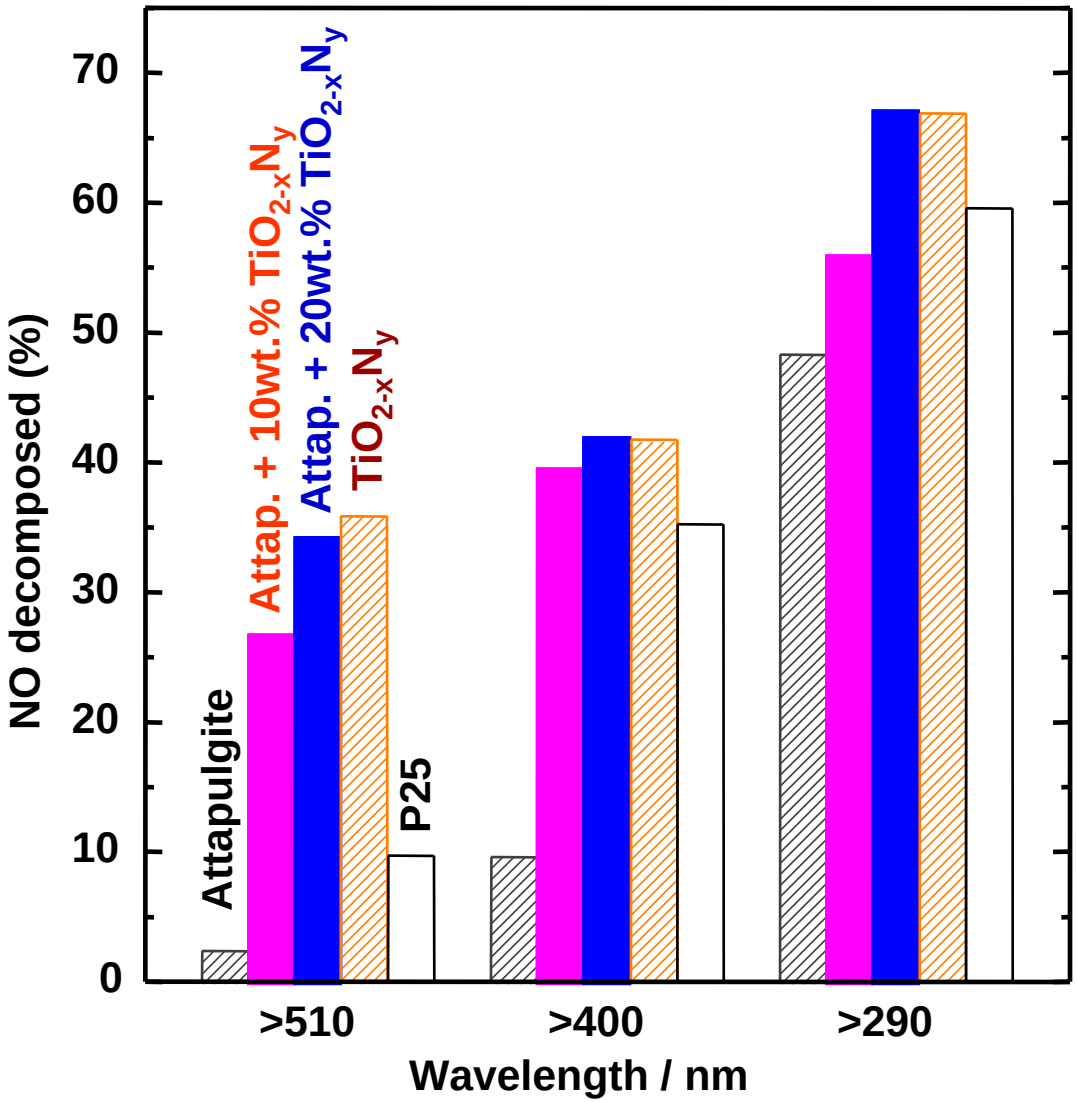

NO destruction with $TiO_{2-x}N_y$/attapulgite composites

Persistent Photocatalyst of Long After Glaw Phosphor/$TiO_{2-x}N_y$ Composites

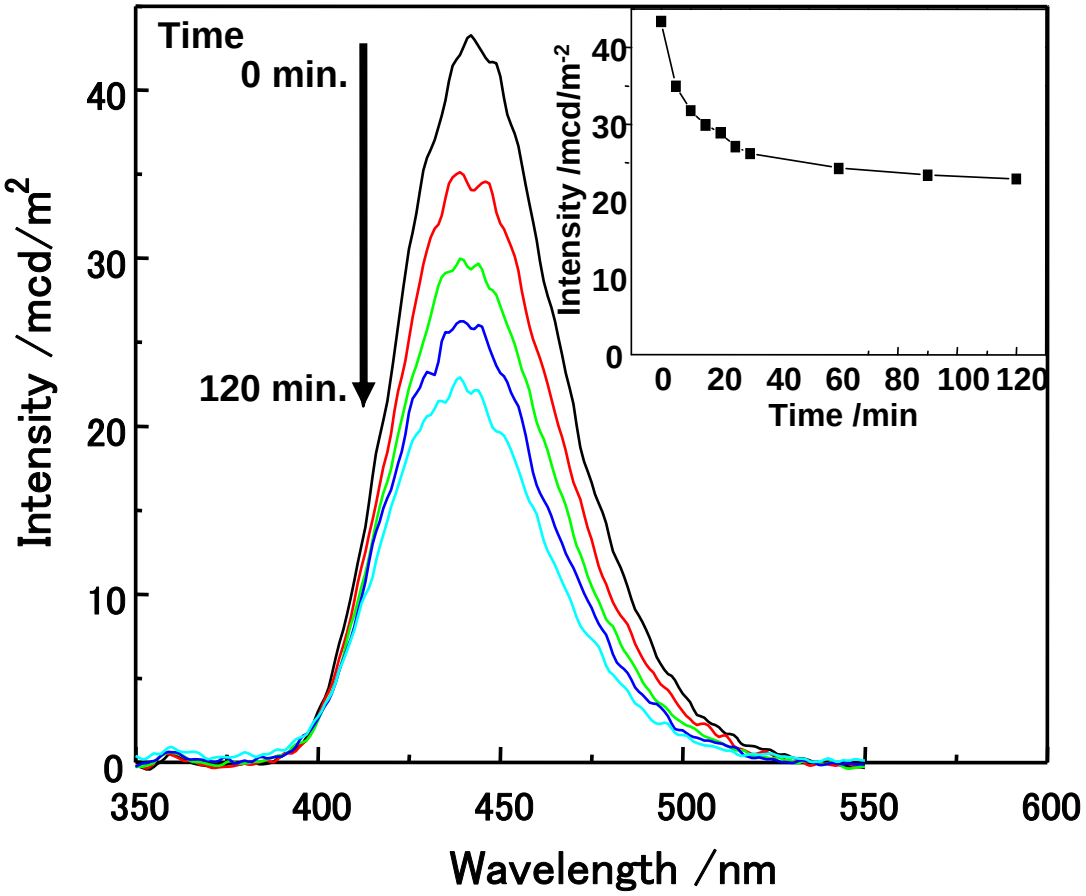

Emission spectra of $CaAl_2O_4$:(Eu,Nd)

Emission Spectrum & Diffuse Reflectance Spectra

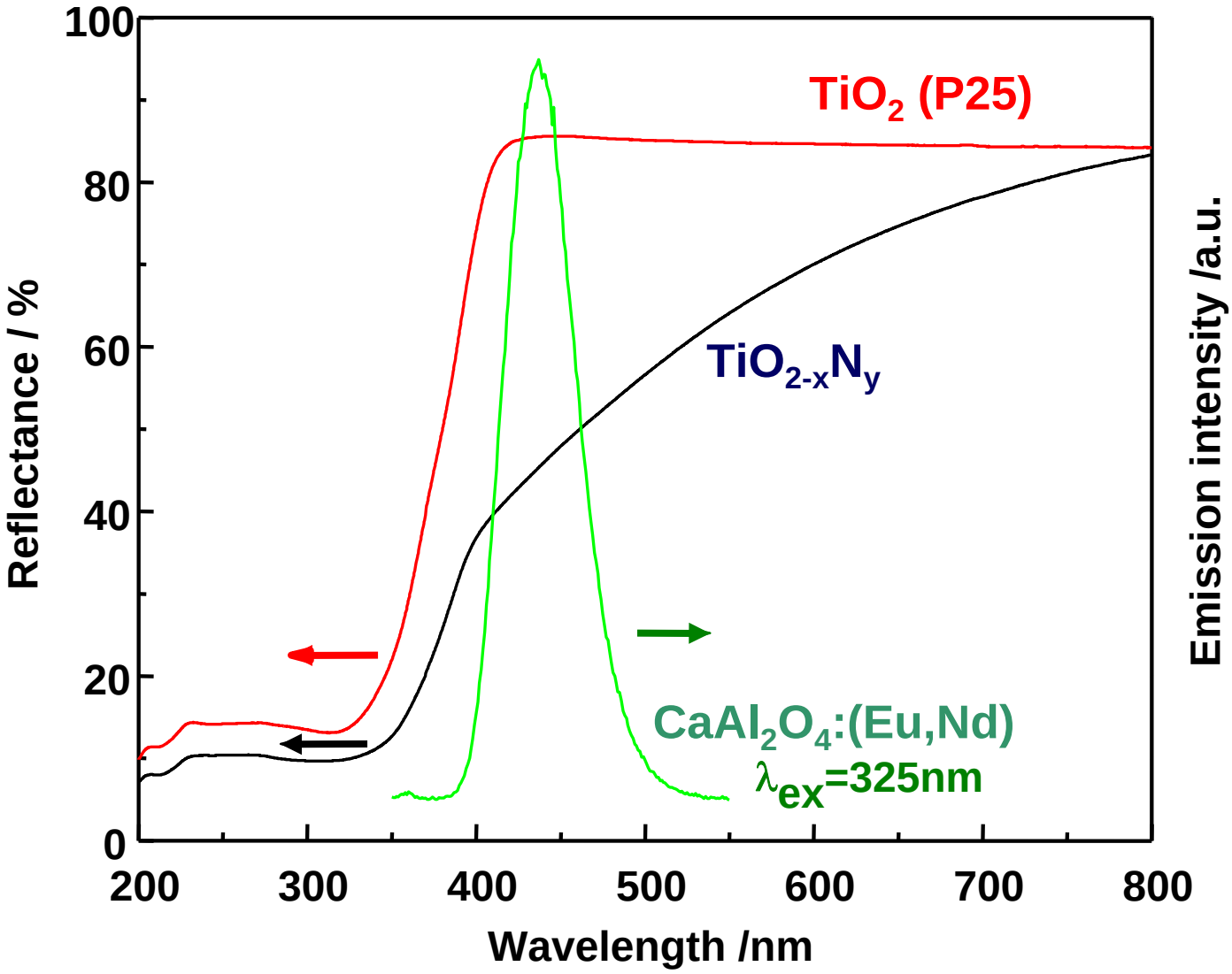

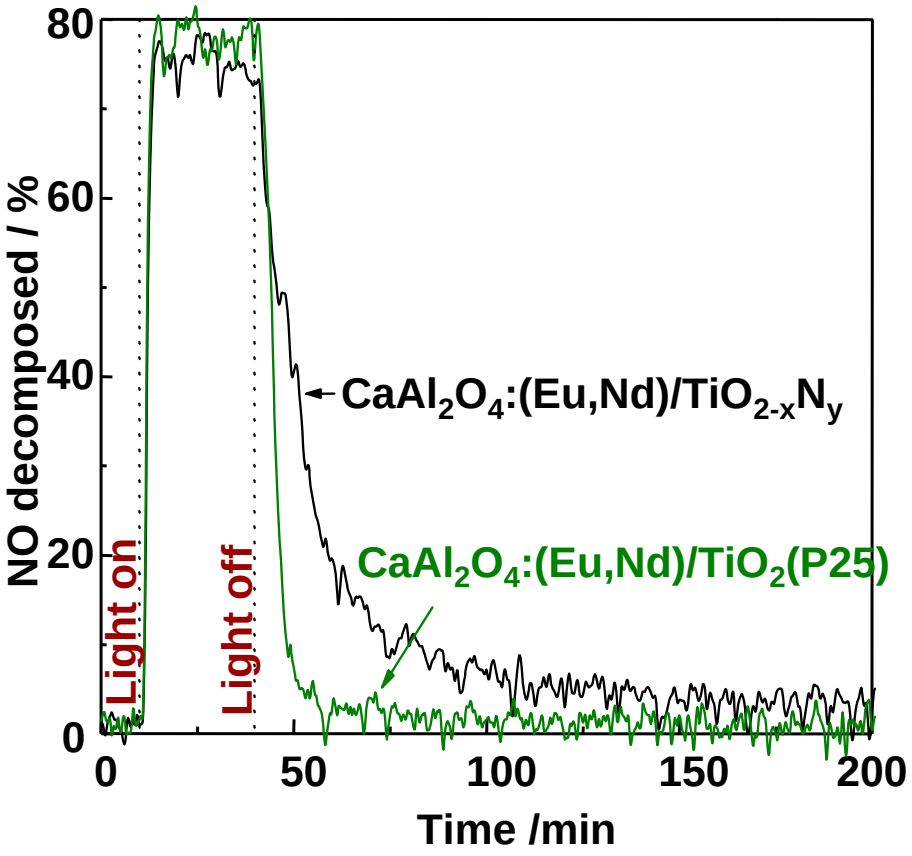

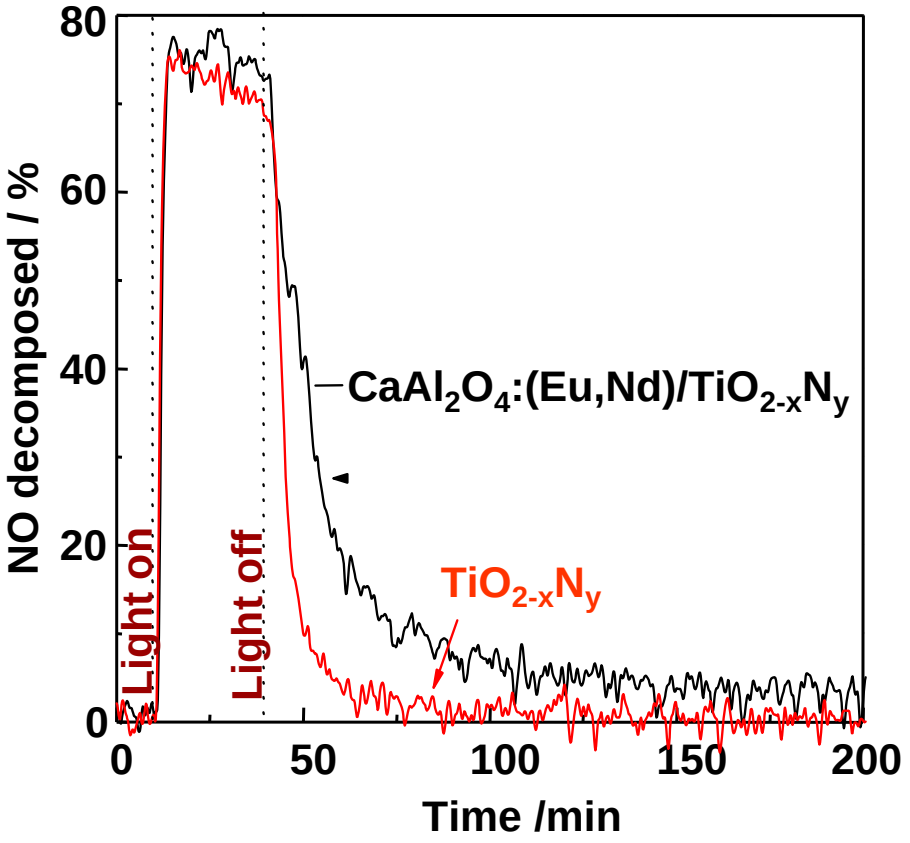

Oxidative destruction of NO under irradiation of UV light and after turning off the light

Conclusions

- Visible light responsive nitrogen-doped titania with high specific surface area were prepared by solvothermal reactions in mixed solution of $TiCl_3$-hexamethylenetetramine.

- Nitrogen-doped titania showed excellent photocatalytic activity for the environmental clean-up.

- The photocatalytic performance of nitrogen-doped titania could be improved by co-doping with higher valence metal ions and/or lower valence anion, and coupling with semiconductors, clay minerals and long afterglaw phosphors.

- Panoscopic Assembling of Ceramic Materials for High Performance Application
- Design and Development of Photocatalyst for Environmental Clean-up
- Design and Development of Ceria-based Inorganic UV-shielding Materials for Human Health
- Conclusion

Damages Caused by UV-ray

Solar spectra

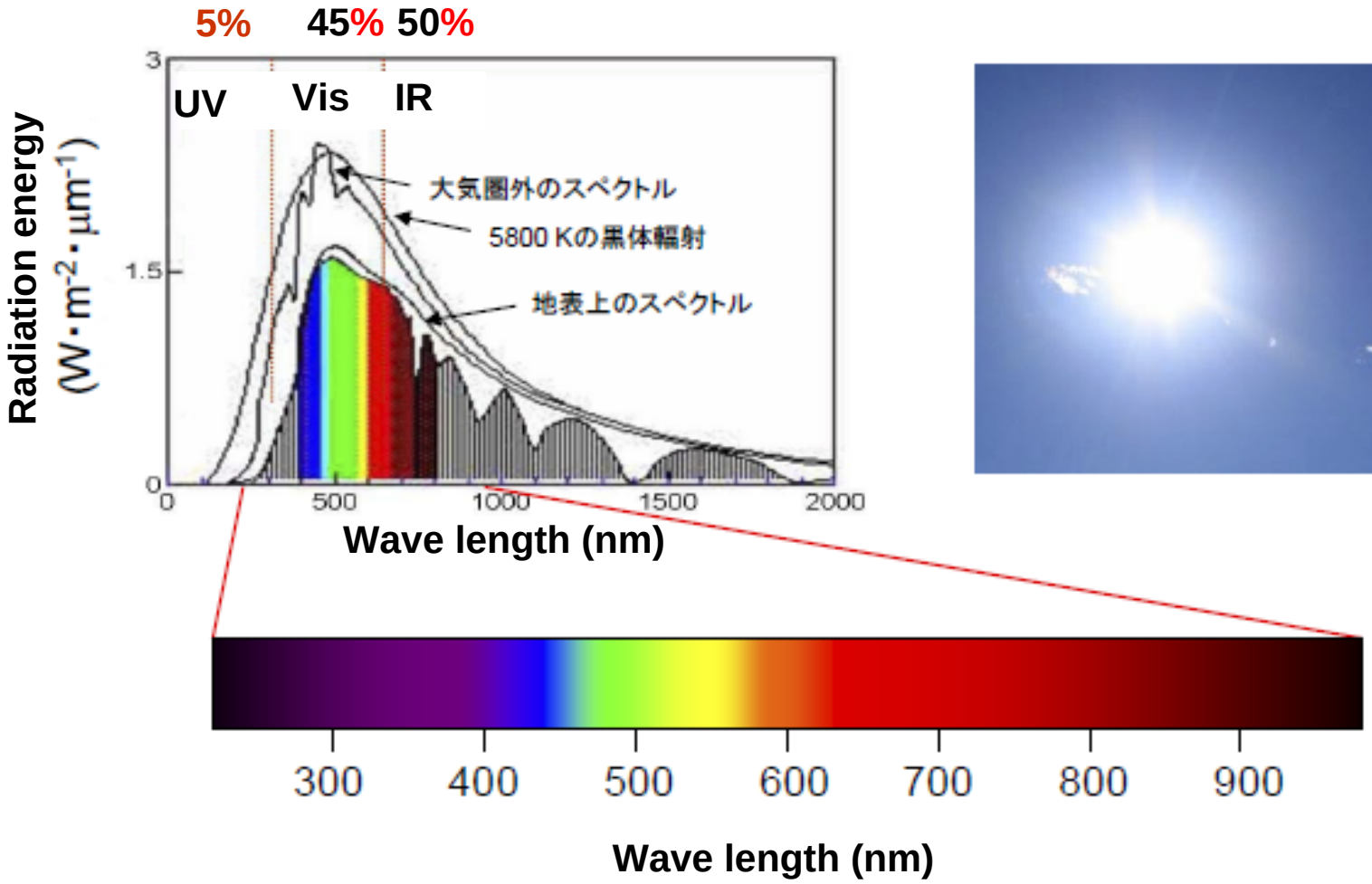

Degradation of organic materials

$$-CH_2CHClCH_2Cl- \xrightarrow{\text{UV light}} CH_2CHClCH{=}CH- + HCl$$

↓ Burning

Dioxin

Discoloration of painting

Damages to human

Sunburn

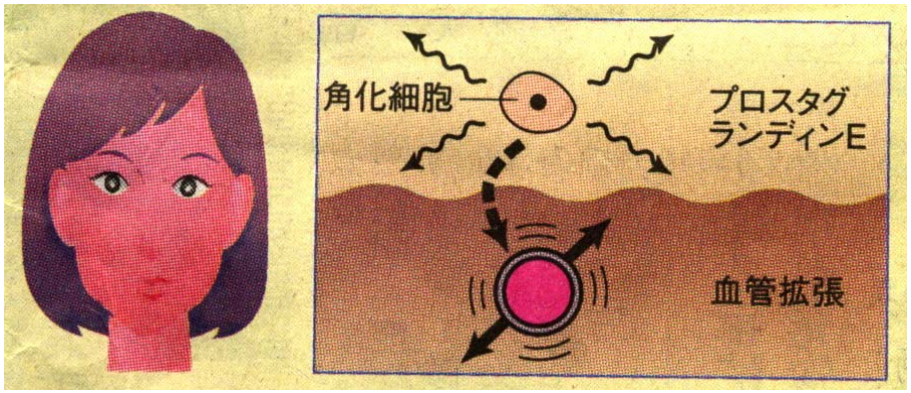

Suntan

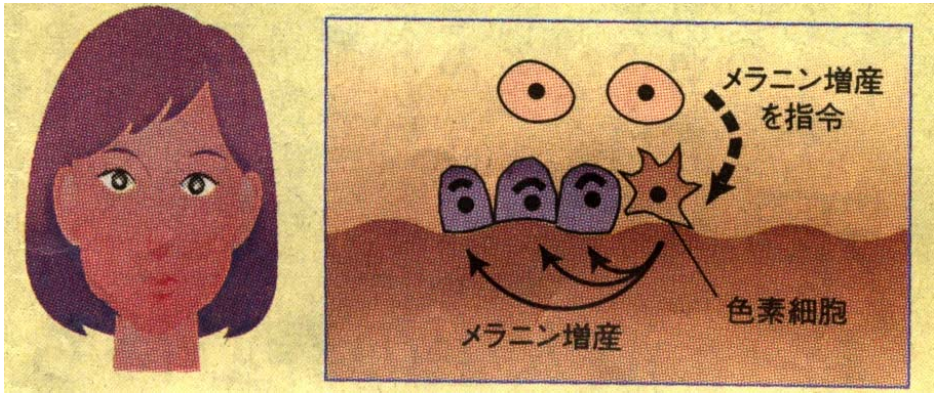

Acceleration of aging

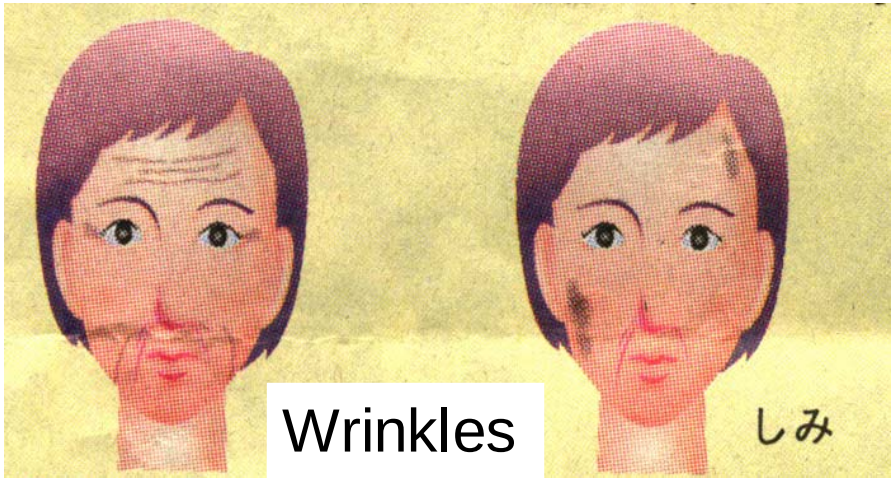

Cancer

Structures of Typical Organic UV- absorbents

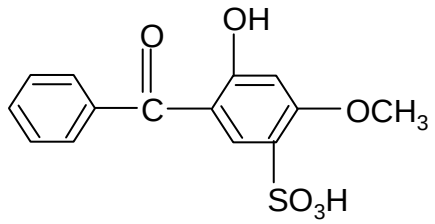

HMBSA
2-hydroxy-4-methoxy-benzophenone-5-sulfonic acid

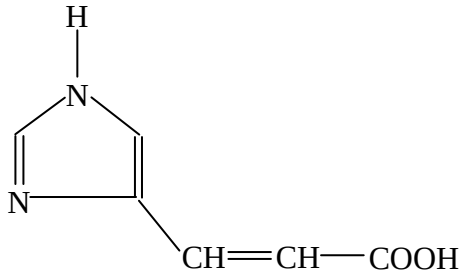

UA
urocanic acid

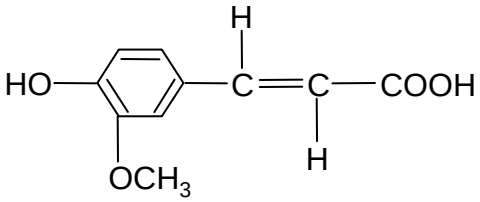

HMCA
***trans*-4-hydroxy-3-methoxycinnamic acid**

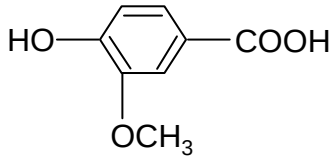

HMBA
4-hydroxy-3-methoxybenzoic acid

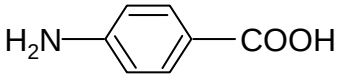

PABA
***p*-aminobenzoic acid**

Organic UV absorbents

Advantage Excellent UV absorption ability

Disadvantage Being absorbed in the body through the skin, raising safety concerns

Stable and safe inorganic UV absorbents

Design of Inorganic UV-shielding Materials

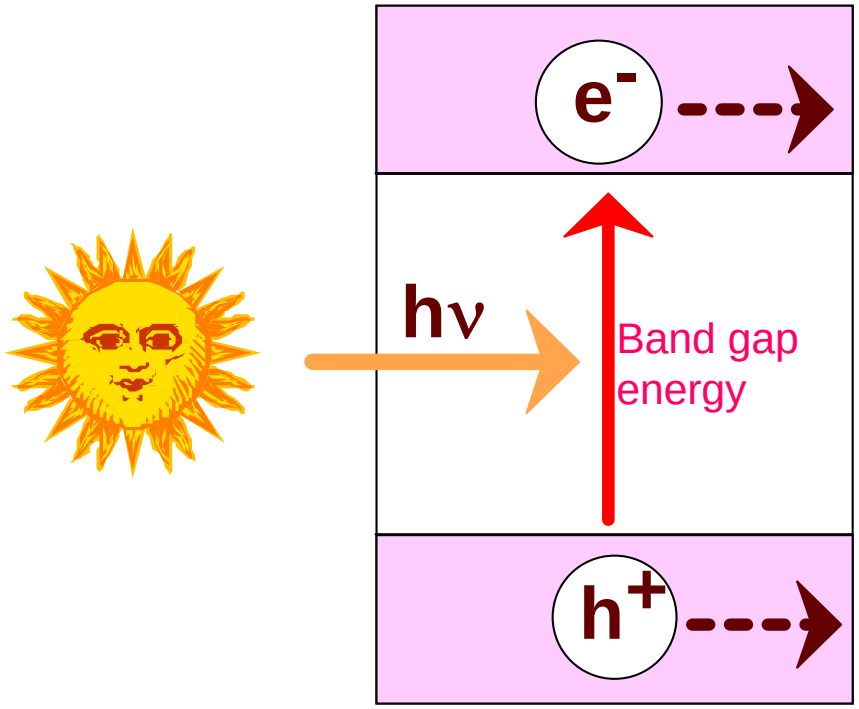

Photocatalyst

Solar battery

Optical sensor

UV-shielding material

Light absorption by the electric transition of semiconductor

$E_b = h\nu = hc/\lambda$

Cut off UV light (λ < 400 nm) ➡ Band gap energy: ca. 3 eV

Light scattering

a) Geometrical scattering region ($d >> \lambda$)

$s \propto 1/d$

b) Mie scattering region ($d \sim l$)

$s \propto d^2 f(d/\lambda, n)$

The scattering becomes greatest when $d=\lambda/2$

c) Rayleigh scattering region

$s = K_3 d^6/\lambda^4$

The scattering is in proportion to the particle size to the sixth power

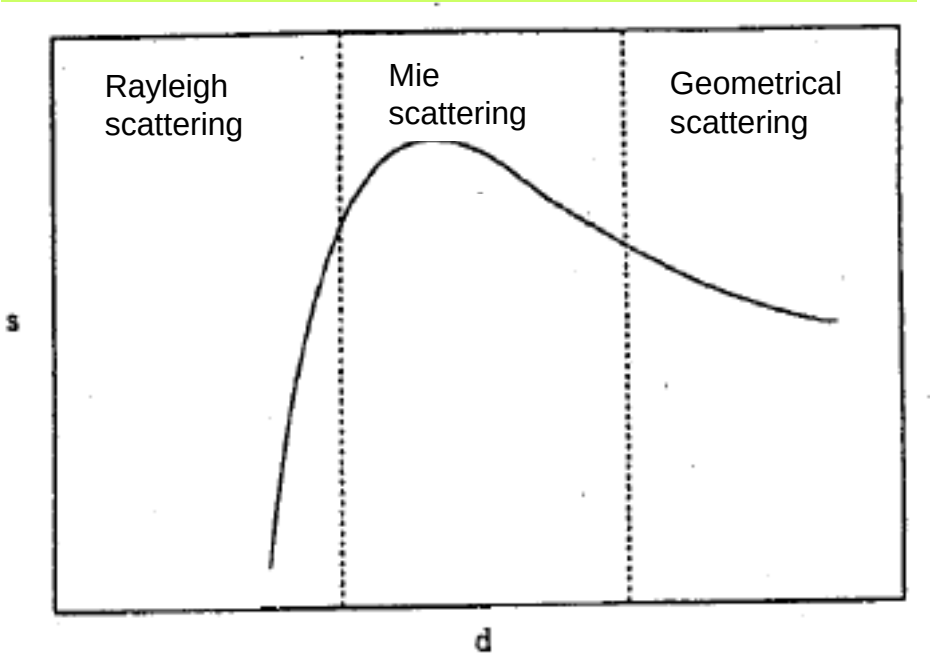

Improving the transparency in visible light range

Depression of light scattering

Decreasing the particle size to less than half of wavelength

(Nanoparticles of d<20 nm become quite transparent)

Typical Inorganic UV-shielding Materials

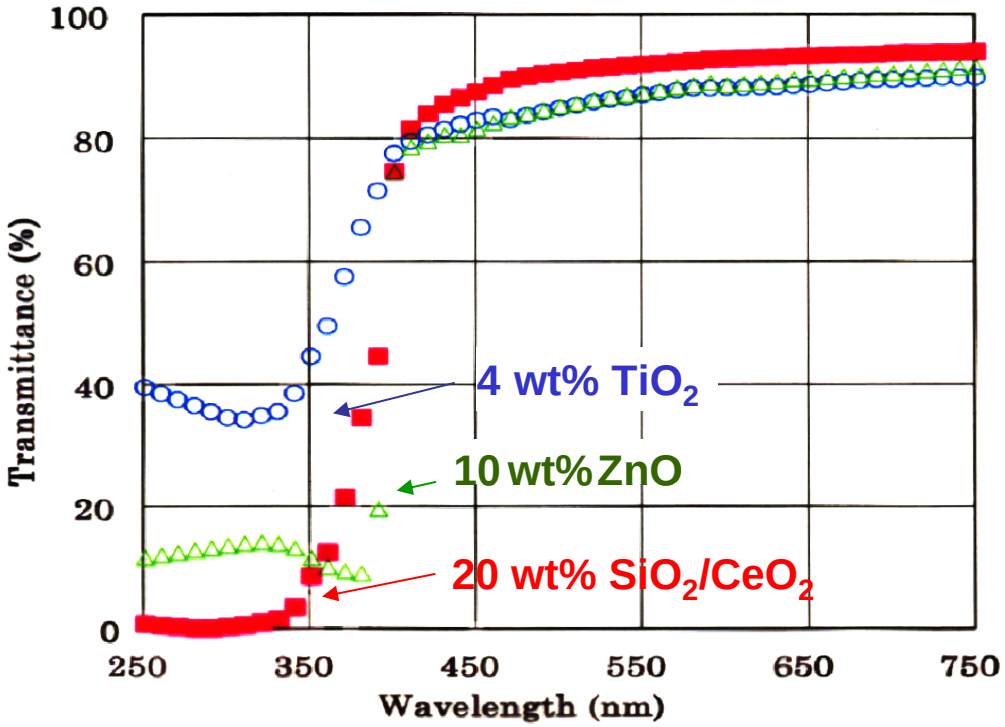

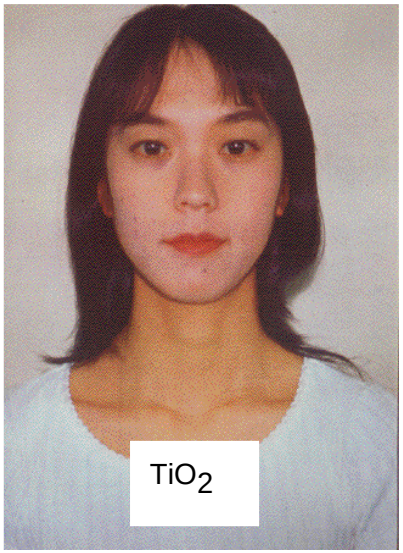

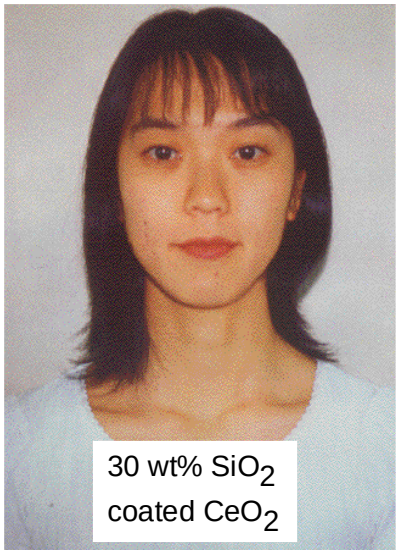

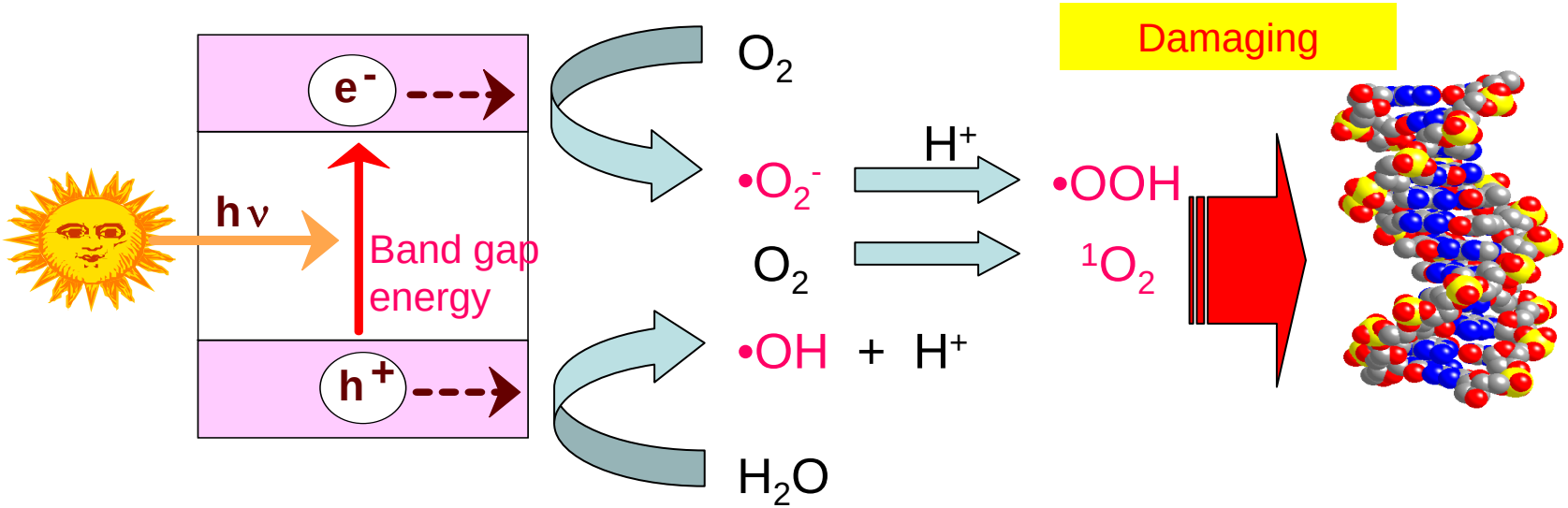

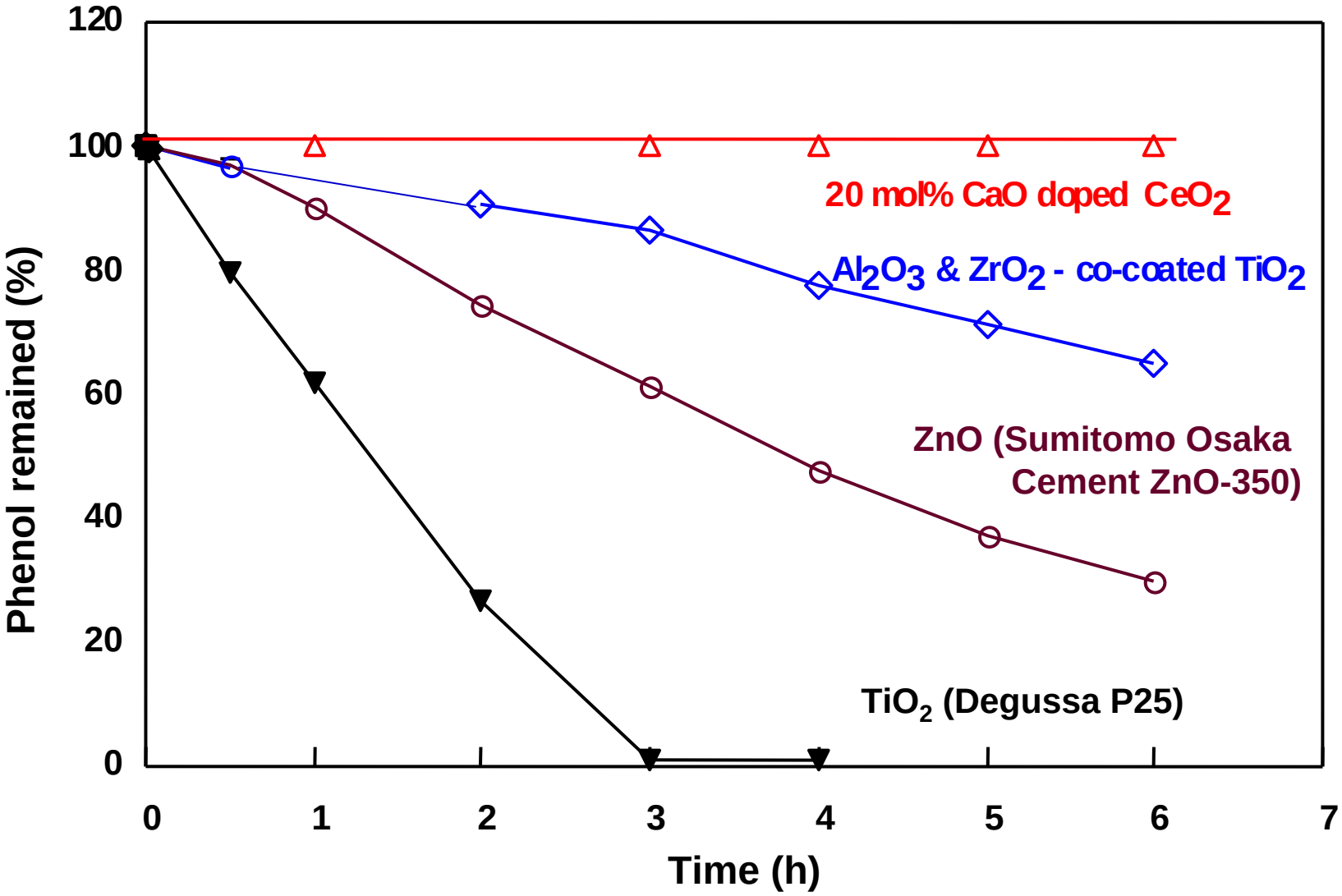

Photocatalytic decomposition of phenol by irradiation of UV-ray from a 100 W high pressure UV lamp to 0.5 mM phenol aqueous solutions dispersed various samples

Damages of DNA under UV irradiation in the presence of UV-shielding materilas

Plasmid DNA pUC 18
1 μ L
+
Sample
(0.01g/9mL-water)
20 μ L

Light intensity
2.8 mW/cm^2 (250nm)
3.5 mW/cm^2 (360nm)

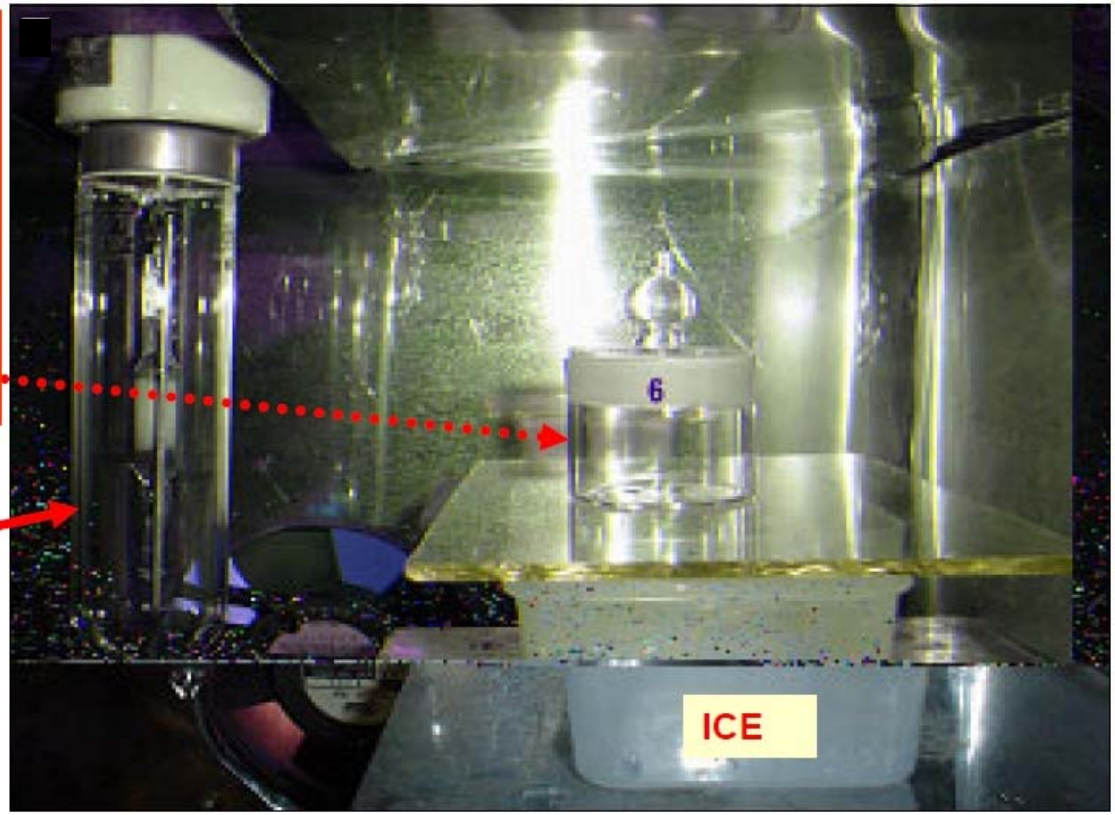

75W Hg-lamp

Plasmid DNA pUC 18 (A_{260}/A_{280}=1.76)
Molecular weight 2,686 bp
NIPPON GENE

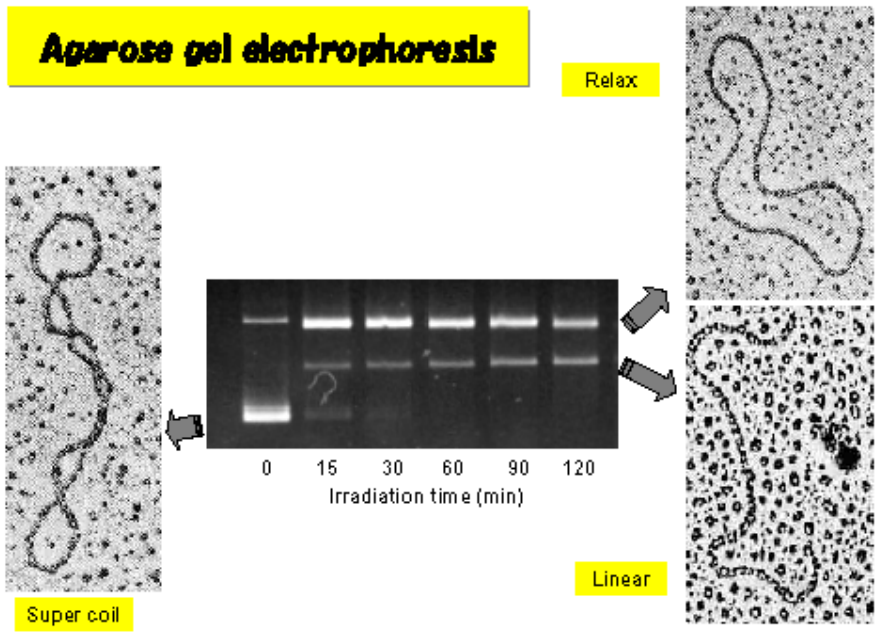

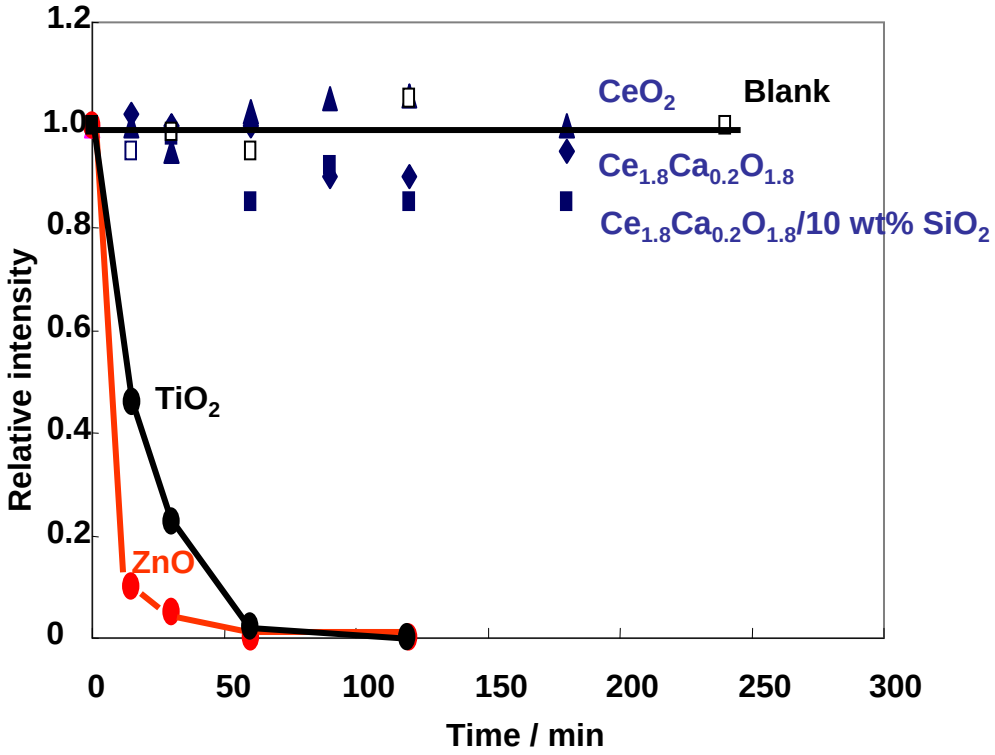

Analysis of DNA configulation

Time dependence of the relative intensity of super coil configulation

H. Hidaka, H. Kobayashi, T. Koike, T. Sato and N. Serpone, DNA damage photoinduced by cosmetic pigments and sunscreen agents under solar exposure and artificial UV illumination, *J. Oleo Sci.*, *55*, 249-261 (2006).

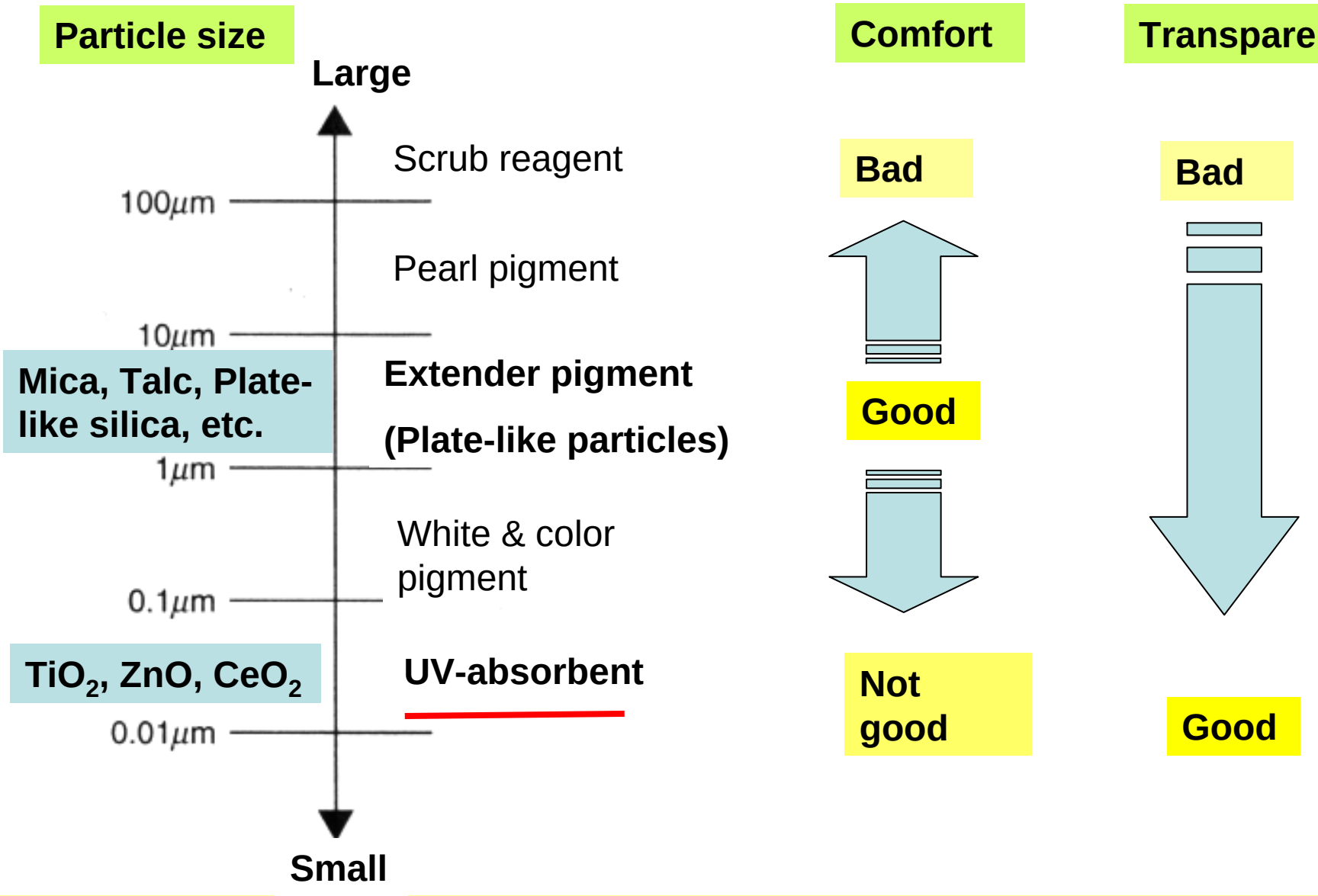

Size, comfort and transparency of the powder when applied on the skin

UV-shielding Material Composite

- **UV-absorption ability**
- **Good comfort**

- **TiO_2 nanoparticle**
- **ZnO nanoparticle**

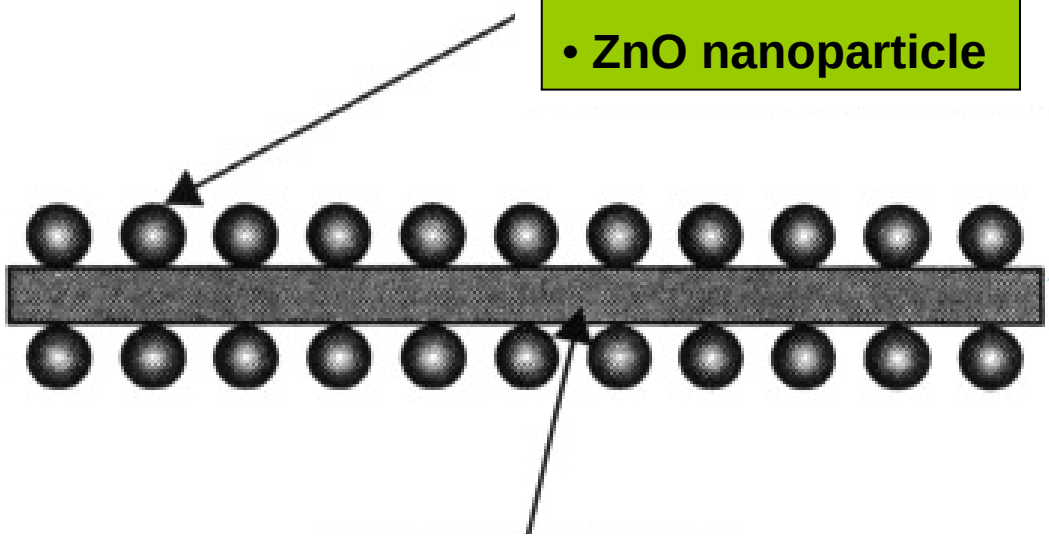

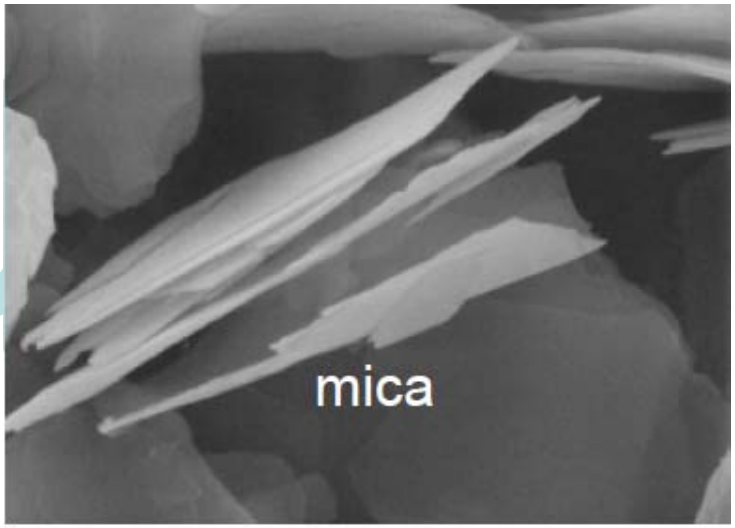

- **Mica**
- **Talc**
- **Plate-like SiO_2**

（No UV-absorption ability）

Decreasing UV-shielding ability

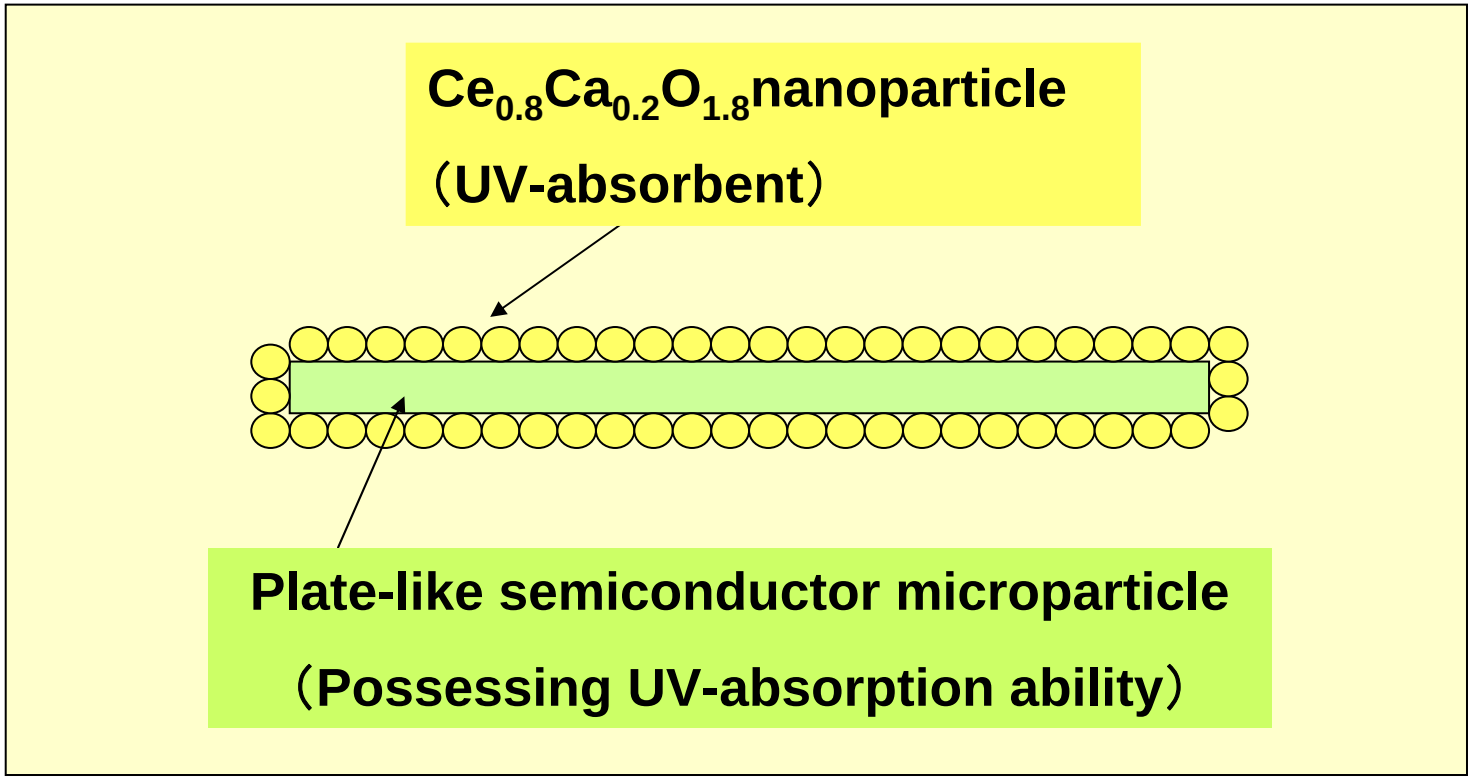

Panoscopic assembling of ceria nanoparticles
Using plate-like semiconductor

- Excellent comfort when applied on the skin
- Excellent coverage ability

Enhance the comfort as well as UV-shielding ability

Mica

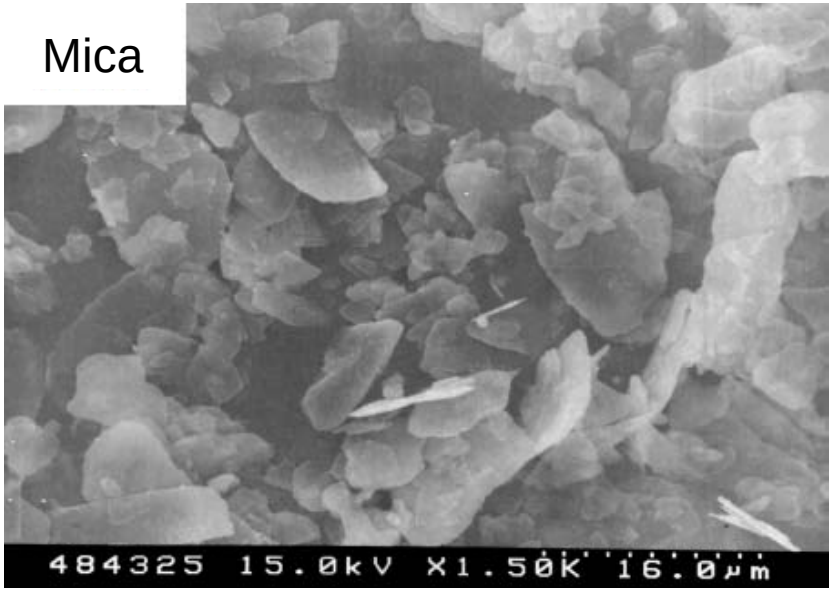

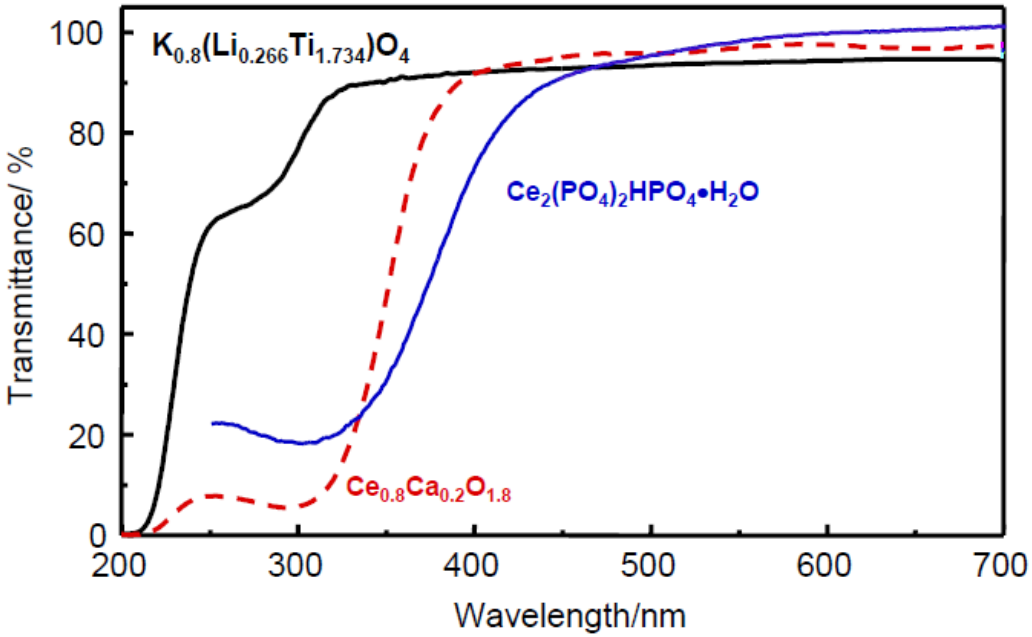

$K_{0.8}(Li_{0.266}Ti_{1.734})O_4$ (E_{bg} = ca. 3.5 eV)

$Ce_2(PO_4)_2HPO_4•H_2O$ (E_{bg}=ca. 2.6 eV)

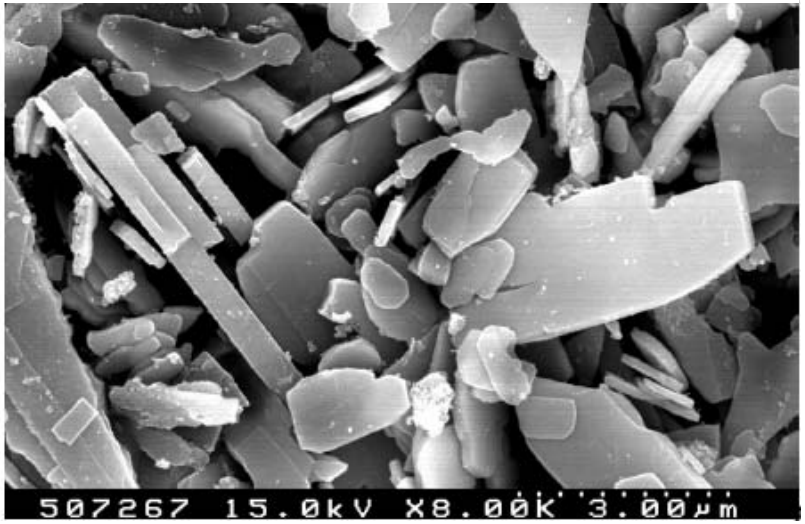

Preparation of plate-like titanate microparticle/calcia-doped ceria nanoparticle composites

i. Coprecipitation method

ii. Sol-gel method

iii. Layer-by-layer assembling method

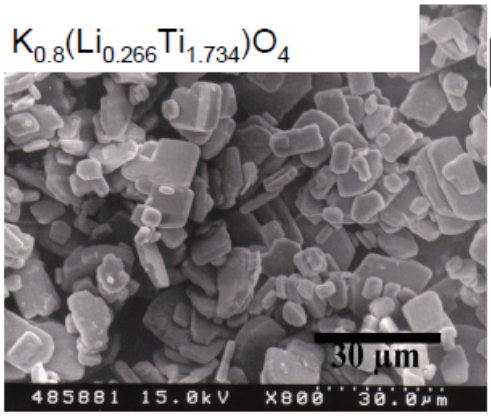

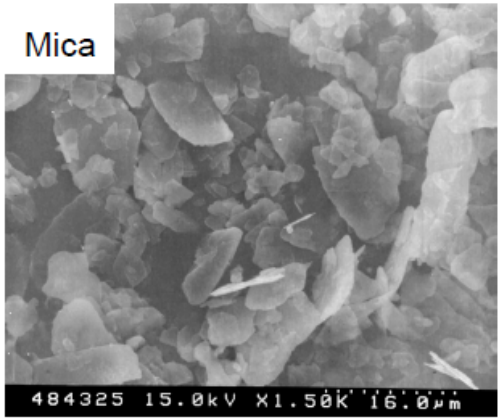

Distilled water 150 ml
40°C

1 M $CeCl_3$-$CaCl_2$
100 ml

50 ml/h

3 M NaOH
100ml

40°C, pH 6 - 12

$CeCl_3 + 3NaOH \rightarrow Ce(OH)_3 + 3NaCl$

Hydroxide gel
prepcipitation

2 M H_2O_2
20ml

50 ml/h

40°C, pH 6 - 12

$2\ Ce(OH)_3 + H_2O_2 \rightarrow 2\ CeO_2 + 4\ H_2O$

$Ce_{1-X}M_XO_{2-(2-n/2)X}$
(n=2,3)

Centrifugation
Washing (H_2O, MeOH)

Calcination at
700°C for 1 h

Preparation of $K_{0.8}Li_{0.27}Ti_{1.73}O_4/Ce_{0.8}Ca_{0.2}O_2$ nanocomposites

Isoelectric points of plate-like titanate and calcia-doped ceria nanopaericles prepared at various pHs

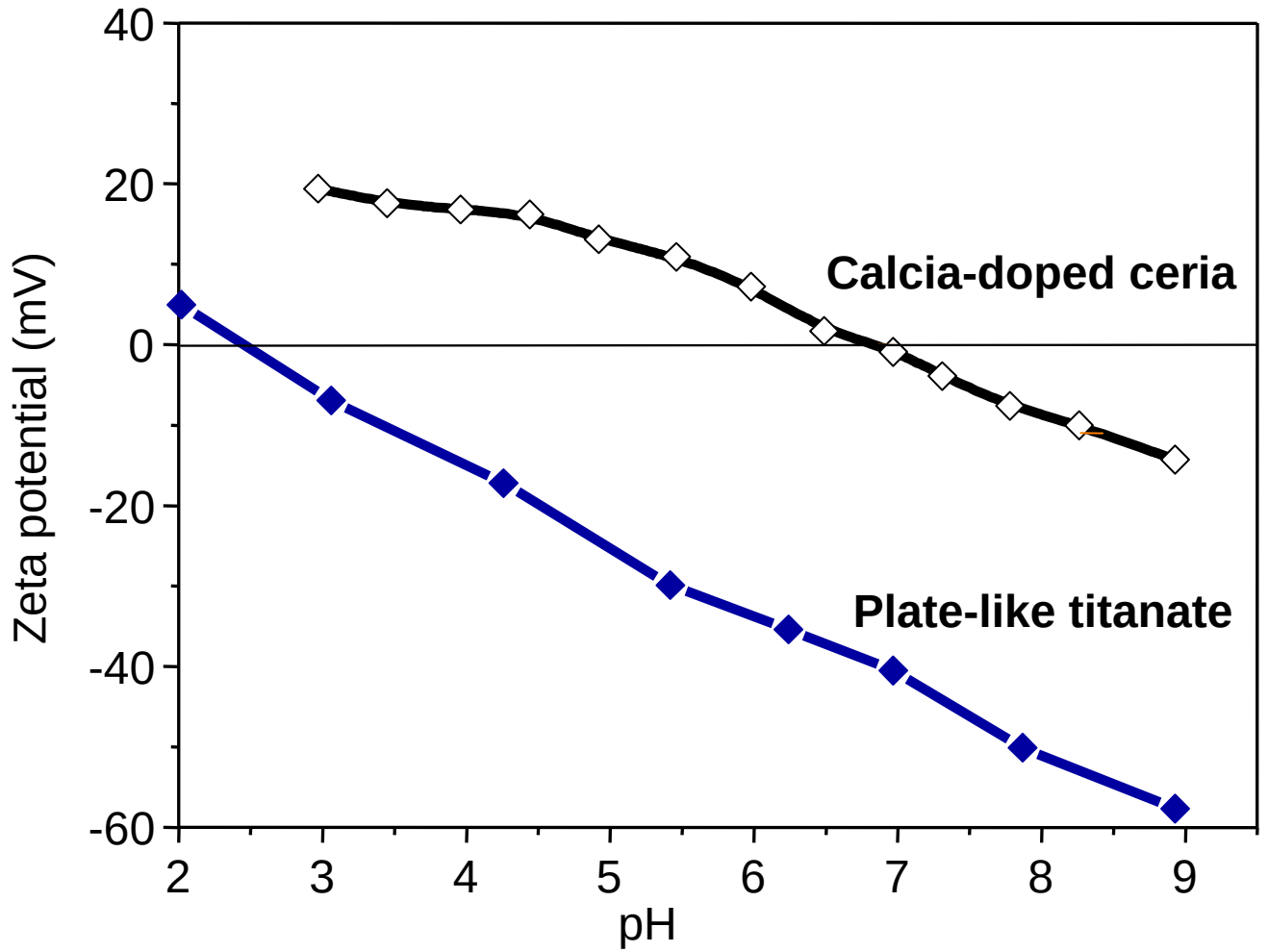

Preparation of ceramic composites using hetero coagulation

$K_{0.8}(Li_{0.27}Ti_{1.73})O_4$

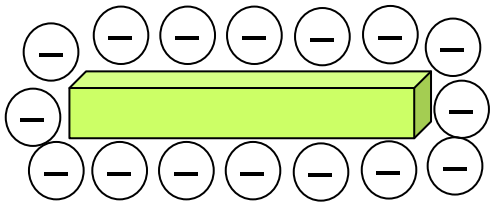

pH control

Surface charge control

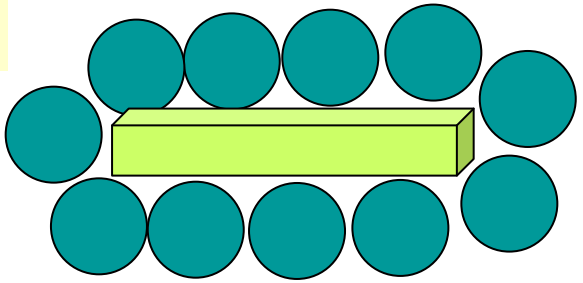

CeO_2

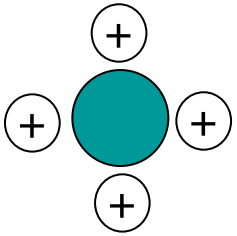

$K_{0.8}(Li_{0.27}Ti_{1.73})O_4$ CeO_2

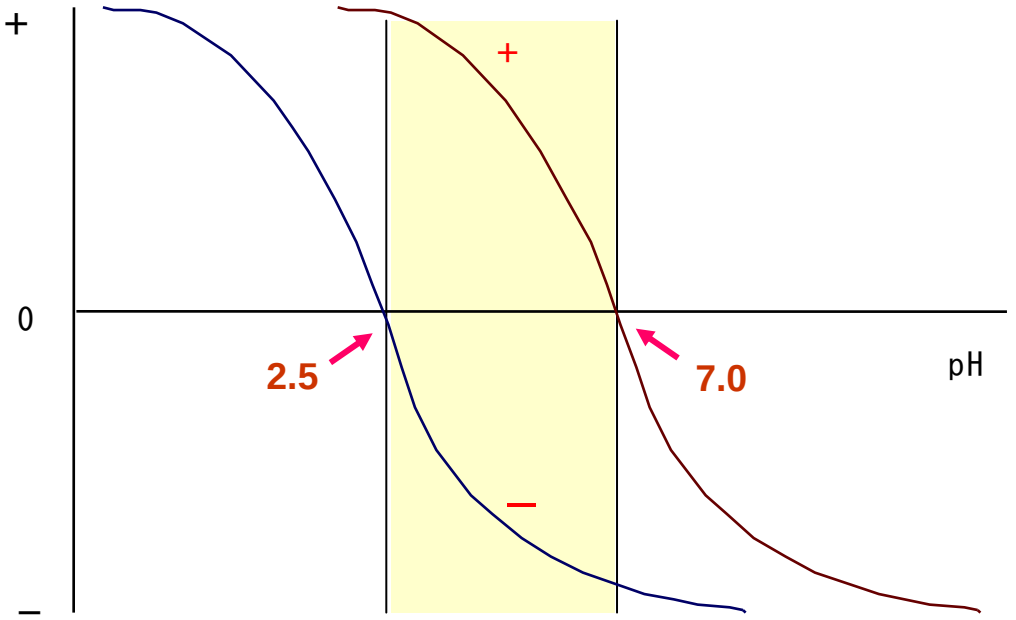

Plate-like titanate (PLT)/calcia-doped ceria (CDC) composites prepared at pH 6.5/12.0 with different CDC concentrations

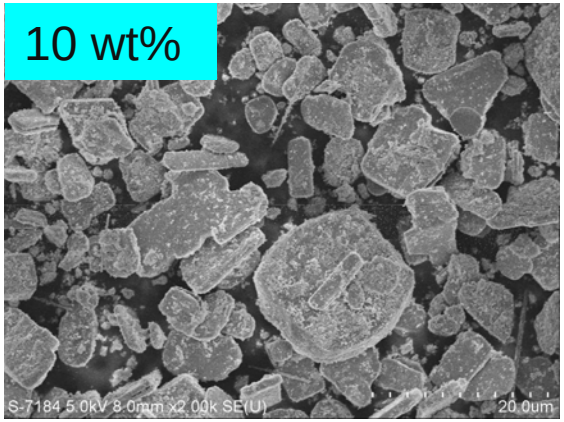

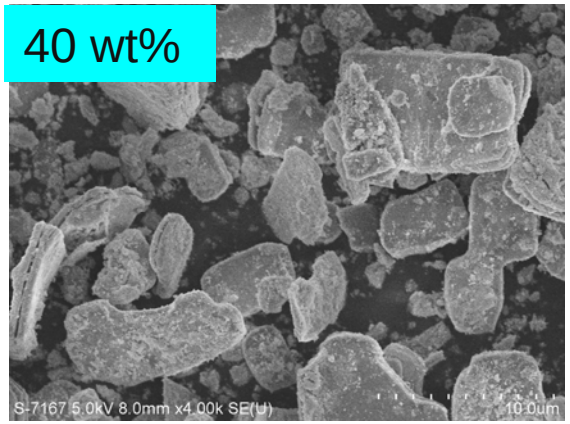

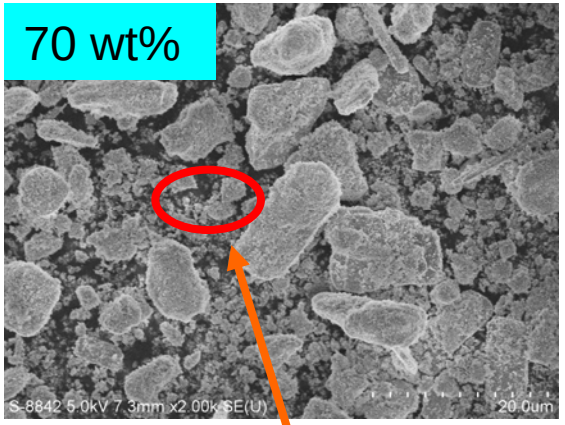

pH=6.5

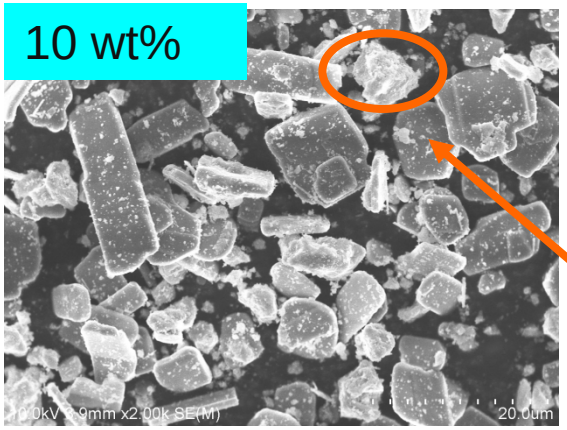

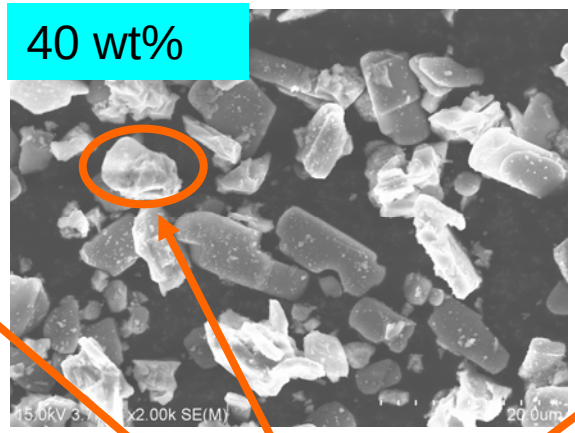

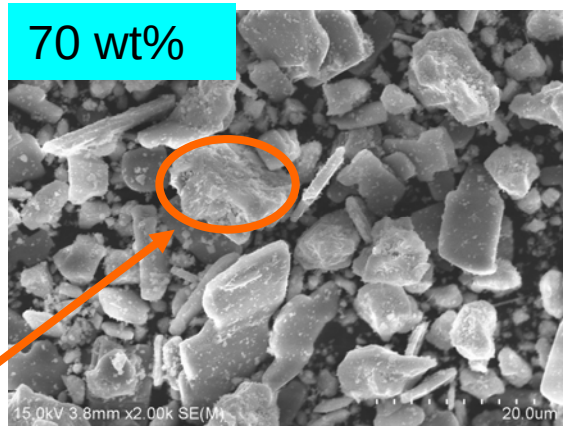

pH=12.0

Agglomeration of CDC

Morphology of plate-like titanate (PLT)/calcia-doped ceria (CDC)

PLT before coating by CDC

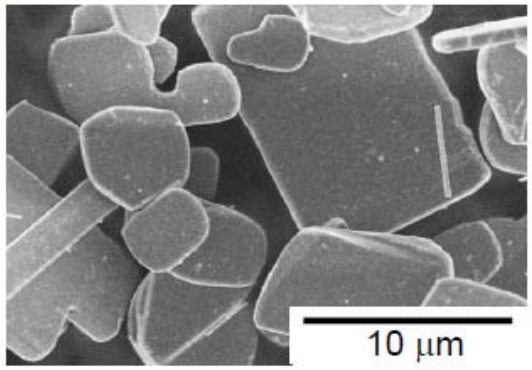

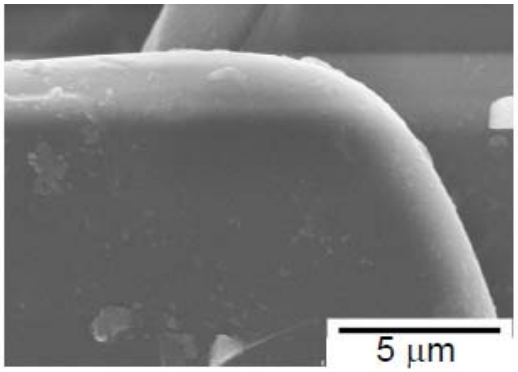

PLT after coating by CDC at pH 6.5

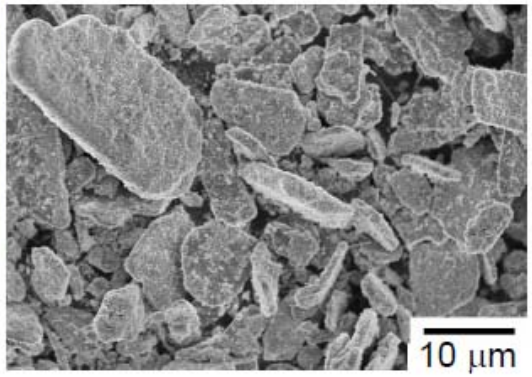

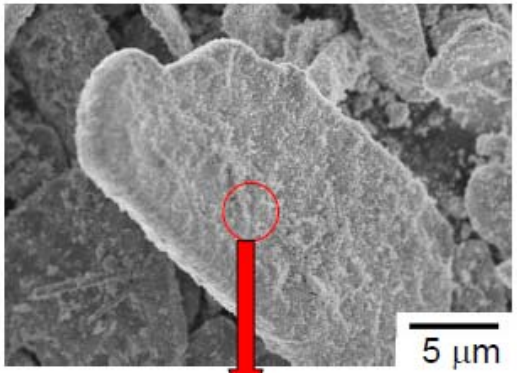

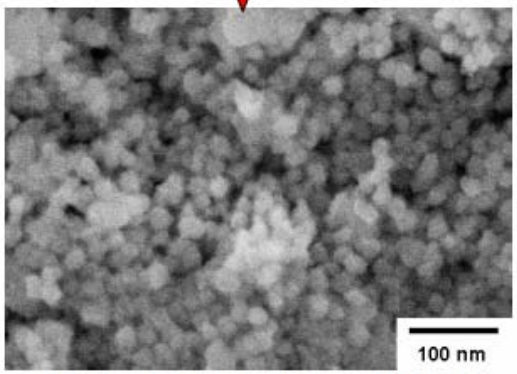

Diameter: 15-20 nm

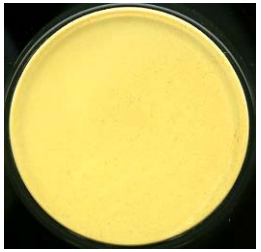

700 °C
1 h

Micro/nano panoscopic assembling

Equipment: KES-SE friction tester (KES KATO TECH CO., LTD)

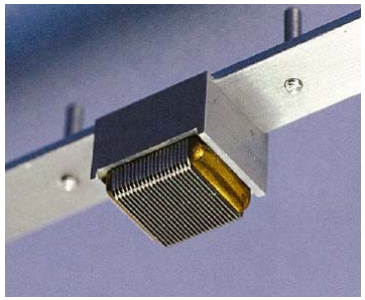

Test condition:
Load weight: 25 g
Slide speed: 0.5 mm/sec
Friction sensor: Piano thread
Substrate: artificial leather

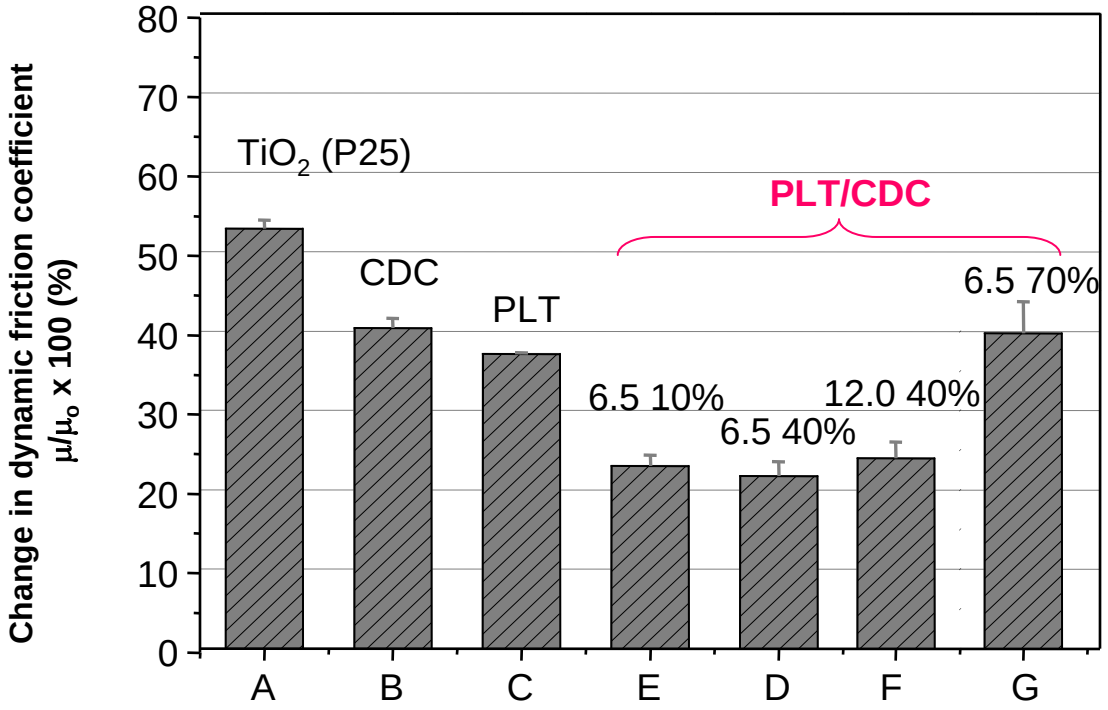

A: P25 (TiO_2); B: CDC (pH=12.0); C: Plate-like titanate (PLT) before coating; D: PLT/CDC 10 % (6.5); E: PLT/CDC 40 %(6.5); F: PLT/CDC 40 %(12.0); G: PLT/CDC 70% (6.5)

Kinetic friction coefficient of the artificial leather before and after applying various sample powders on.

μ_o: Artificial leather without sample,

μ: Artificial leather applied the sample powder on

PLT before coating

PLT/CDC with proper CDC concentration

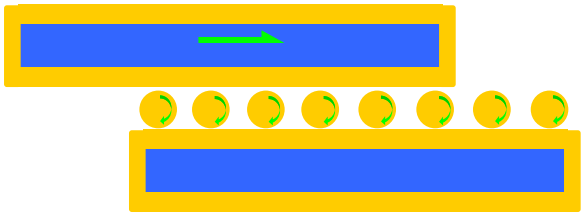

PLT/CDC with high CDC concentration

Slip friction of plate-like particles

Rolling friction of shperical particles

Slip friction of nanoparticles

UV-shielding ability

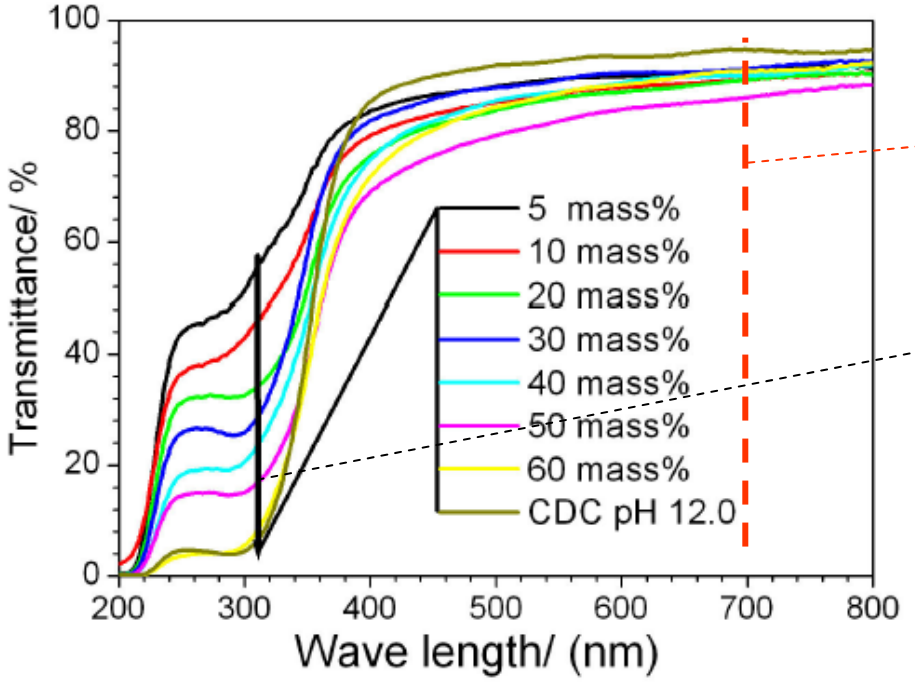

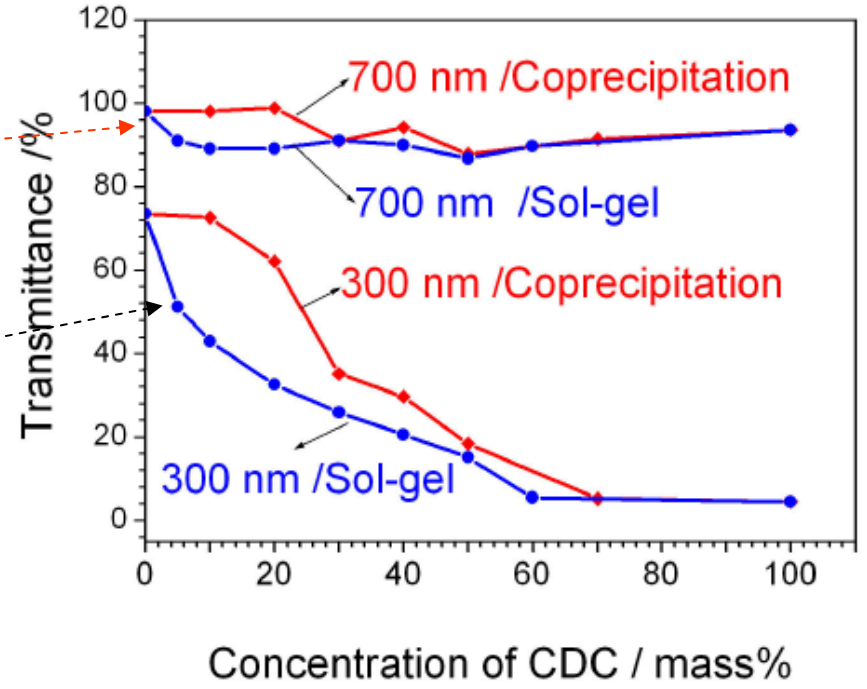

- **The UV-shielding ability of PLT/CDC increased with increasing CDC content**
- **UV-shielding ability of PLT/CDC prepared by sol-gel method was higher than that by co-precipitation method**

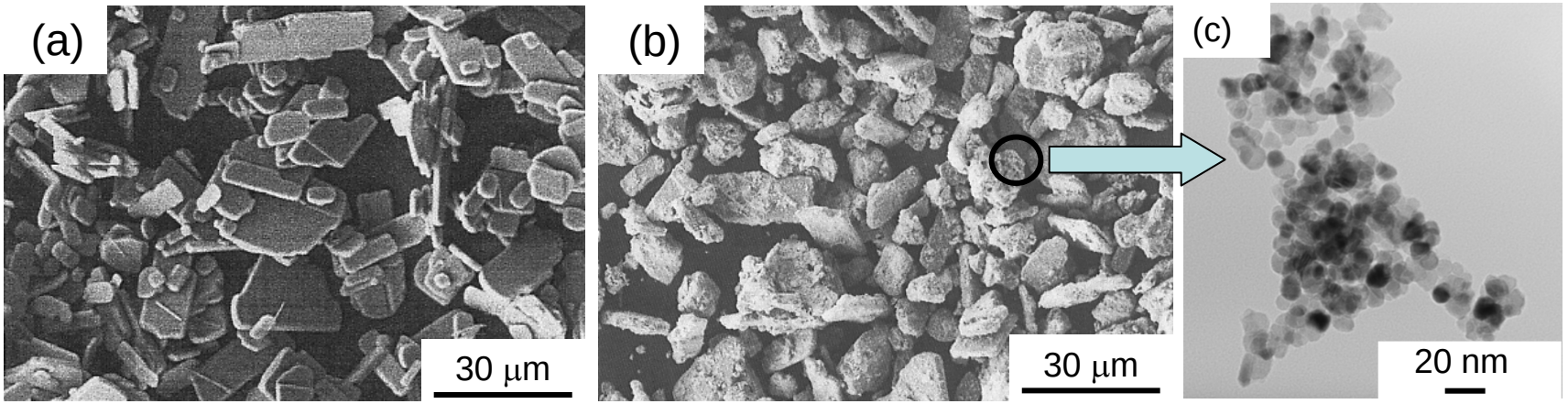

$K_{0.80}Ti_{1.73}Li_{0.27}O_4$

As-prepared $K_{0.80}Ti_{1.73}Li_{0.27}O_4$/
50 wt% $Ce_{0.8}Ca_{0.2}O_{1.8}$

$Ce_{0.8}Ca_{0.2}O_{1.8}$

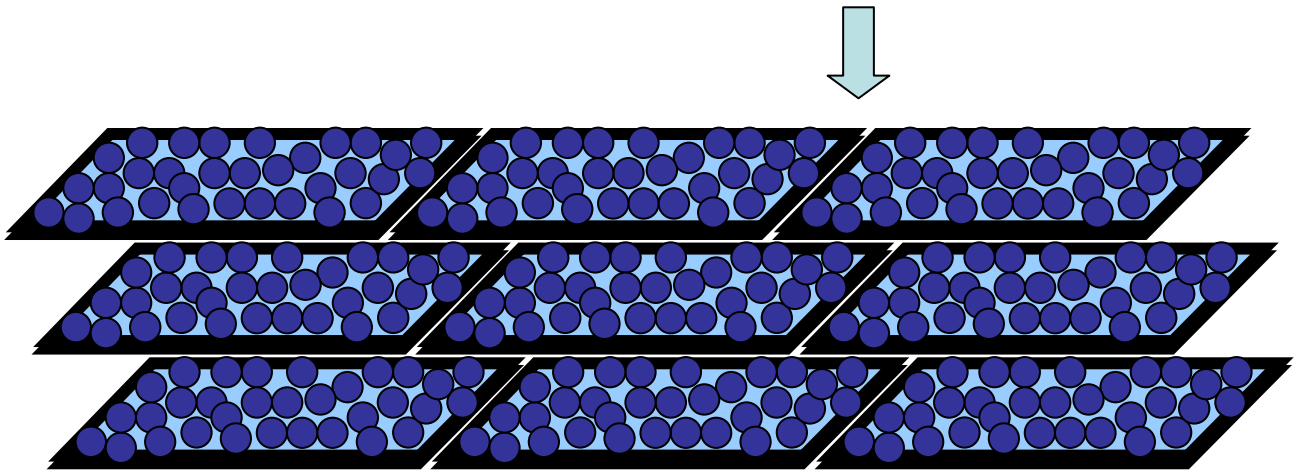

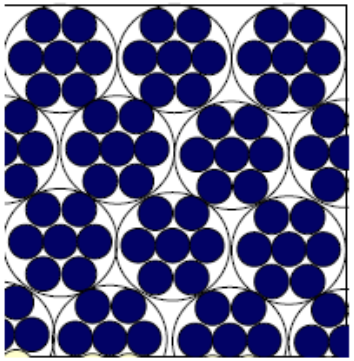

Improving the comfort and covering ability of inorganic nanoparticles by the panoscopic assembling using plate-like particles

- Nanocomposites of plate-like $K_{0.81}Li_{0.27}Ti_{1.73}O_4$ microparticles/ $Ce_{0.8}Ca_{0.2}O_{1.8}$ nanoparticles were prepared by coprecipitation method.

- Panoscopic assembling of $Ce_{0.8}Ca_{0.2}O_{1.8}$ nanoparticles with plate-like $K_{0.81}Li_{0.27}Ti_{1.73}O_4$ was useful to improve the comfort when applied to the skin as well as the UV-shielding performance.

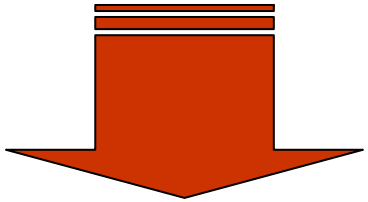

New Inorganic UV-shielding Materials

with Safe, Comfort and Excellent UV-shielding Ability

- Panoscopic Assembling of Ceramic Materials for High Performance Application
- Design and Development of Photocatalyst for Environmental Clean-up
- Design and Development of Ceria-based Inorganic UV-shielding Materials
- Conclusion

- Nanocomposites of nitrogen-doped titanina nanoparticles and semiconductor possessing different band gap, clay mineral such as attapulgite, long afterglow phosphor, etc. showed excellent photocatalytic performance for environmenta clean-up.

- Nanocomposites of $Ce_{0.8}Ca_{0.2}O_{1.8}$ nanoparticles and plate-like semiconductors possessing UV-shielding ability, such as $K_{0.81}Li_{0.27}Ti_{1.73}O_4$ showed excellent UV-shielding performance for human health as well as excellent comfort when applied to the skin.